東北医科薬科大学

審査学位論文（博士）

氏名（本籍）	ジョ　コウ 徐　興　（中国）
学位の種類	博士（薬科学）
学位記番号	博薬学第 25 号
学位授与の日付	令和 6 年 3 月 8 日
学位授与の要件	学位規則第 4 条 1 項該当
学位論文題名	Importance of core fucosylation in regulating neuroinflammation （神経炎症の調節におけるコアのフコシル化の重要性）
論文審査委員	主査　教 授　山口　芳樹
	副査　教 授　細野　雅祐
	副査　教 授　顧　建国

Importance of core fucosylation in regulating neuroinflammation

令和 6 年 3 月

東北医科薬科大学大学院薬学研究科

徐　興

Contents

1. Introduction

Core fucosylation is catalyzed explicitly by α1,6-fucosyltransferase (Fut8) that transfers a fucose residue from guanine nucleotide diphosphate (GDP)-fucose onto the innermost asparagine-linked *N*-acetylglucosamine (GlcNAc) through an α1,6-linkage in mammals (1). The biosynthesis of core fucosylation demands donor substrate GDP-fucose, which can be synthesized by two distinct pathways: the *de novo* pathway and the salvage pathway (Fig. 1) (2). Under normal conditions, the *de novo* pathway produces up to 90% of GDP-fucose. When this pathway is disrupted, the salvage pathway compensates for the shortfall of GDP-fucose (3,4). L-Fucose is a six-deoxy hexose monosaccharide that is abundantly present in plants and seaweed (5,6). In mammals, free L-fucose originating from dietary sources or the lysosomal catabolism of glycoproteins can directly serve as a substrate for GDP-fucose synthesis via the salvage pathway (4,7). The produced GDP-fucose is subsequently transported into the lumen of the Golgi apparatus through the GDP-fucose transporter and subjected as the donor substrate for fucosyltransferases, such as Fut8 that catalyzes core fucosylation (Fig. 1) (8).

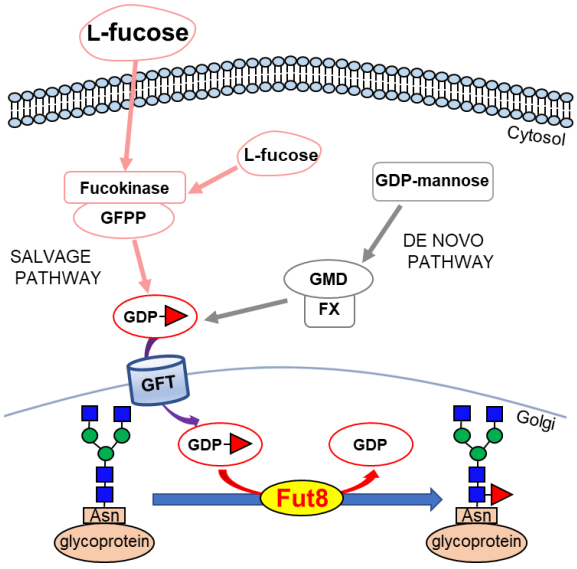

Figure 1. A synthetic pathway for GDP-fucose synthesis.

Therefore, exogenous L-fucose potentially enhances core fucosylation levels. The variety of core fucosylation is intimately involved in the pathophysiological processes of numerous diseases, including pulmonary emphysema (9), schizophrenia (10), cancers such as hepatocellular carcinoma (11), non-small cell lung cancer (12), pancreatic carcinoma (13), and antibody-dependent cellular cytotoxicity (ADCC) (14,15).

It has been well-established that neuroinflammation is a normal immune response resulting from numerous pathological injuries, including ischemia, toxins, infection, and trauma in the central nervous system (CNS) (16). Neuroinflammation cascades primarily depend on the activation of microglial cells, which are the CNS-resident innate immune cells stemming from the yolk sac macrophages (17-19). Additionally, upon pathological stimuli or neuronal insults, microglia secrete proper concentrations of immune mediators, such as interleukin-6 (IL-6), IL-1β, nitric oxide (NO) and tumor necrosis factor-alpha (TNF-α) to coordinate neuroinflammation (19,20). Among numerous pro-inflammatory cytokines, IL-6 is the most pivotal cytokine for acute-phase responses (14). It can be produced by various types of cells, including microglia, astrocytes, neurons, macrophages, and B cells (21,22). IL-6 is a multifunctional and pleiotropic cytokine and is associated with multiple sclerosis (23), experimental autoimmune encephalomyelitis (24), perioperative neurocognitive disorders (25) and depression (26). In the CNS, proinflammatory IL-6 signaling is mainly mediated via trans-signaling with soluble IL-6 receptor (sIL-6R) that subsequently constitutes a complex with glycoprotein 130 (gp130) and activates downstream Janus kinase (JAK)/signal transducer and activator of transcription (STAT) signaling pathway (27,28). Previous studies have confirmed that many types of cytokine and immune receptors, such as TGF-β1 receptor (9), B cell receptor (BCR) (15), T cell receptor (TCR)

(15,29), integrin α3β1 (30) and epidermal growth factor (EGF) receptor (31), contain core fucosylation that differently regulates their biological functions.

Fut8 homozygous knockout ($Fut8^{-/-}$) mice exhibit a schizophrenia-like phenotype with a decrease in working memory (10) and long-term potentiation (32). Curiously, patients suffered from a complete loss of core fucosylation due to biallelic Fut8 mutations (33) showed growth retardation, and severe developmental and neurological impairment, which were quite similar to the abnormal phenotypes observed in the $Fut8^{-/-}$ mice (9,10). While the pathophysiology of schizophrenia has not yet been fully elucidated, several studies suggest that neuroinflammation leading to glial dysfunction could contribute to the pathogenesis of schizophrenia (34,35). Our previous study revealed that core fucosylation negatively regulated the sensitivity of glia to inflammatory stimuli (36). The initial activation status of glial cells in the neuroinflammation induced by lipopolysaccharide (LPS) was significantly enhanced in the $Fut8^{-/-}$ mice, compared with wide-type ($Fut8^{+/+}$) mice. Notably, the degree of neuroinflammation in the Fut8 heterozygous knockout ($Fut8^{+/-}$) mice ranged between that of $Fut8^{+/+}$ and $Fut8^{-/-}$ mice, presumably due to haploinsufficiency of Fut8. Consistently, the $Fut8^{+/-}$ mice exhibited greater sensitivity to cigarette smoke-induced emphysema than the $Fut8^{+/+}$ mice (37).

In the present study, we explore the importance of core fucosylation and its participation in neuroinflammation, utilizing the bacterial artificial chromosome (BAC)-based human IL-6 gene (*hIL6*) driven firefly luciferase reporter transgenic mice that we previously generated (21). After crossbreeding the *hIL6*-BAC-*Luc* mice with the $Fut8^{+/-}$ mice, we obtained the Fut8::*hIL6-Luc* compound transgenic mice. Using this mouse strain, we quantitatively monitored the neuroinflammation induced by LPS. We found that the $Fut8^{+/-}$::*hIL6-Luc* mice showed a higher neuroinflammatory response than $Fut8^{+/+}$::*hIL6-Luc* transgenic mice. Exogenous L-fucose ameliorated the LPS-induced

neuroinflammatory responses, including glial cell activation and several cytokine expressions in the $Fut8^{+/-}$ mice. Considering that L-fucose is a natural and non-toxic food ingredient, such as seaweed (38), the present study proposes its potential utility for the treatment or prevention of neuroinflammation.

2. Materials and methods

2.1. Antibodies and reagents

The experiments were performed using the following antibodies and reagents: Biotinylated *Lens Culinaris Agglutinin* (LCA) (J207), which preferentially recognizes core fucose (39), was obtained from J-oil Mills (Tokyo, Japan). The anti-Fut8 antibody (sc-271244) was obtained from Santa Cruz Biotechnology. The antibodies against GAPDH (G9545), α-Tubulin (T6199), the peroxidase-conjugated secondary antibody against mouse IgG (AP124P) and LPS purified from Escherichia coli O111:B4 (L2630) were from Sigma. The anti-Phospho-JAK2 (#3771), anti-JAK2 (#3230), anti-Phospho-Akt (#4060), anti-Akt (#9272), anti-Phospho-STAT3 (#9145), anti-STAT3 (#9139) antibodies and the secondary antibody about HRP-conjugated goat against rabbit (#7074) were purchased from Cell Signaling Technology. The antibody against ionized calcium-binding adaptor molecule-1 (Iba-1) (019-19741) was from Wako (Tokyo, Japan). The anti-gp130 (#A304-929A) and anti-IL-6R (#MA5-29721) antibodies were from Thermo Fisher Scientific. Ab-Capcher MAG2 was purchased from ProteNova (Higashi Kagawa, Japan). ABC kit (PK-4000) was from Vector Laboratories. The goat anti-rabbit antibody Alexa Fluor 488 (A-11008) was from Invitrogen. L-Fucose (F0065) was purchased from TCI (Tokyo, Japan).

2.2. Animals

All animal experiments complied with protocols approved by the Animal Care and Use Committee of the Graduate School of Pharmaceutical Sciences, Tohoku Medical and Pharmaceutical University. $Fut8^{+/+}$ littermates and $Fut8^{+/-}$ mice were obtained by intercrossing the ICR genetic background heterozygous mice (10). Generation and analysis of the *hIL6*-BAC-*Luc* reporter transgenic mice were previously reported (21). The $Fut8^{+/-}$ mice were mated with *hIL6*-BAC-*Luc* reporter

transgenic mice to produce Fut8$^{+/+}$::*hIL6-Luc* and Fut8$^{+/-}$::*hIL6-Luc* compound transgenic mice. All experiments were conducted with 5-6 weeks-old male and female mice, male mice with a weight range of approximately 28-30 g and female mice with a weight range of approximately 26-28 g. Mice were housed in groups under standard vivarium conditions (12-h light/dark cycle, lights on from 7:00 to 19:00, 22 ± 2 °C ambient temperature, and 55 ± 5% relative humidity) with free access to food and water. The mice were orally administrated L-fucose twice a day via oral gavage, with incremental doses of 4 mg/day, 12 mg/day and 36 mg/day. The dosage of L-fucose was determined based on our previous study (40) and clinical research (4), where approximately 10-20 mg/day per 30 g body weight of L-fucose was found to be effective.

2.3. Cell culture

The mouse microglia cell line BV-2 was kindly gifted by Professor Elisabetta Blasi (University of Modena and Reggio Emilia, Modena, Italy) and cultured in DMEM with 10% fetal bovine serum under a humidified atmosphere at 37 °C and 5% CO_2.

2.4. Establishment of Fut8-KO cells

The pSpCas9(BB)-2A-GFP (PX458) plasmid was obtained from Addgene (plasmid ID: 48138). BV-2 Fut8-KO cells were constructed via guide RNA (5'-ATTCGTCCACAACCTTGGC-3') targeted to mouse Fut8 gene localized adjacent to Cas 9 in the pSpCas9(BB)-2A-GFP vector. The plasmid was electroporated into the BV-2 according to the manufacturer's instructions (Amaxa® cell line Nucleofector® kit V, Lonza). After 48 h post-transfection, GFP-positive cells were sorted using FACSAria II (BD Bioscience) and subsequently seeded into 96-well plates to establish single clones. Genomic DNA was amplified via PCR using the following primers: Forward primer (5'-

CCCCATTGTAGACAGCCTCC-3'); Reverse primer (5'-ACAGTCTCTAGGGTCTGGAAC-3'), and sequenced with the reverse primer.

2.5. HPLC separation of nucleotide sugars

Nucleotide sugars were purified from brain tissues using the protocol (41,42). The column was Interstil ODS-4, 4.6 × 250 mm, 3 μm particle size and flow rate was set to 0.6 ml/min. Buffer A (200 mM triethylamine, adjusted pH to 6.0 with acetic acid) was used for equilibration, and buffer B (80% of A plus 20% acetonitrile) was used as an eluent. Elution gradient in the long column was conducted as follows: 100% buffer A for 35 min, 0% to 77% linear gradient of buffer B for 40 min, 77% to 100% buffer B for 1 min, 100% buffer B for 14 min, 100% buffer A for 1 min and 100% buffer A for 20 min (42,43). Retention time under separation conditions was approximately 24.54 min for GDP-fucose.

2.6. LC-MS analysis of *N*-glycans from mice hippocampus

N-Glycans from cell membrane proteins from each three-mice hippocampus of $Fut8^{+/+}$ mice, $Fut8^{+/-}$ mice, and $Fut8^{+/-}$ mice treated with 36 mg/day L-fucose, were released with PNGaseF (44), labeled with aminoxyTMT6 reagent (Thermo Fisher Scientific) after the treatment of desialylation with acetic acid and then analyzed by LC-ESI MS, according to previous procedures (45).

2.7. Imaging of luciferase activity *in vivo* and *ex vivo*

In vivo, bioluminescence imaging was conducted using an *in vivo* imaging system (IVIS Lumina Series III; PerkinElmer) as previously described (21). Briefly, the $Fut8^{+/+}$::*hIL6-Luc* and $Fut8^{+/-}$::*hIL6-Luc* transgenic mice were intraperitoneally injected with 75 mg/kg D-luciferin (Promega) 4 h after the intraperitoneal administration of PBS or LPS at a dose of 1 mg/kg. Subsequently, the anesthetized mice were placed in a light-sealed chamber, and the luciferase activity was imaged for 60 s to monitor the neuroinflammation. Regarding the *ex vivo* imaging, the brain tissues were isolated from the

Fut8$^{+/+}$::*hIL6-Luc* and Fut8$^{+/-}$::*hIL6-Luc* transgenic mice euthanized immediately after the administration of D-luciferin, incubating the brain samples in 300 μg/ml D-luciferin in PBS. Luminescence emitted from the cerebral region of the mice was quantified with Living Image software (PerkinElmer).

2.8. Immunoprecipitation

Brain tissues were rapidly extracted on ice, and each 50 mg tissue was homogenized in 500 μl radioimmunoprecipitation assay (RIPA) buffer (20 mM Tris-HCl, pH 7.5, 150 mM NaCl, 2 mM EDTA, 0.1% SDS, 1% NP-40 and 1% protease and phosphatase inhibitors) with φ2.0 Zirconia Beads by Micro Smash MS-100 (Digital Biology), based on the manufacturer's instructions. BV-2 cells were washed with cold PBS for three times, and then lysed with the cell lysate buffer (20 mM Tris-HCl, 150 mM NaCl, pH 7.4, 1% Triton X-100) and 1% protease and phosphatase inhibitors. After centrifugation at 15,000 rpm for 15 min, the supernatants were collected, and the concentration was detected by the BCA protein assay kit (Pierce). For immunoprecipitation, 1.5 μl anti-gp130 antibody was combined with 15 μl Ab-Capcher MAG2 at 4 °C for 2 h with MT-360 Micro Tube Mixer. After washing the mixture three times, the same amounts of proteins (500 μg) from each tissue or cell were immunoprecipitated at 4 °C overnight. And then, these immunoprecipitates were washed twice with PBS and detected by lectin blot and Western blot.

2.9. Western blot and lectin blot

Western blot and lectin blot were performed as follows: proteins (10 μg) or immunoprecipitants (10 μl) were equally loaded into 7.5% or 12% sodium dodecyl sulfate-polyacrylamide gel electrophoresis (SDS-PAGE) at 100 V and then transferred to polyvinylidene difluoride membranes (PVDF, Millipore Sigma) at 10 V for 1 h. After blocking (5% bovine serum albumin (BSA) for lectin

blot / 5% non-fat dry milk for Western blot) for 1 h at RT, the membranes were stained with LCA lectin or indicated primary antibodies at 4 °C overnight. After washing four times, the membranes were incubated with appropriate secondary antibodies. Based on the manufacturer's instructions, immunoreactive bands were detected using an immobilon Western Chemiluminescent HRP Substrate (Millipore).

2.10. Immunofluorescence

After intraperitoneal injection for 4 h, the mice in different experimental groups were deeply anesthetized with pentobarbital sodium and perfused transcardially with 50 ml PBS, afterward intracardially perfused with 50 ml 4% paraformaldehyde (PFA) in 0.01 M PBS, and then removed the brains to 4% PFA for further post-fixed, followed by dehydrating using 10%, 20%, and 30% sucrose respectively. A cryostat sectioned the brains at 40 μm, and the frozen sections were collected in 24-well plates containing PBS. After being permeabilized with PBS containing 0.3% Triton X-100 for 30 min, the brain slices were incubated with PBS-solution containing 3% bovine serum for another 30 min at room temperature, followed by further incubation with anti-Iba-1 (1:200) antibody overnight at a 4 °C room. After that, the brain slices were washed three times with PBS every 10 min, then incubated with a secondary antibody (1:500) for 2 h at room temperature. Finally, the brain slices were marked by DAPI for 10 min in the dark, mounted on glass slides with 30% glycerin, and imaged using ZEISS LSM 900 confocal microscope. The number of Iba-1-labeled microglia was quantified using Image J software.

2.11. RT-PCR and real-time PCR for mRNA expression analysis

RNAs were extracted with TRIzol reagent (Invitrogen), and 1 μg of total RNA was reverse-transcribed into cDNA by PrimeScript RT reagent with gDNA Eraser (Takara) according to the

manufacturer's instructions. The sequences of primers for RT-PCR and real-time PCR are listed in Table 1 and Table 2, respectively. The RT-PCR products were subjected to electrophoresis using 1.5% agarose gels containing ethidium bromide. Real-time PCR assays were executed using a TB Green® Premix Ex Taq™ II (Tli RNaseH Plus) (Takara), and the conditions were as follows: initial denaturation at 95 °C for 30 s, then 40 cycles of denaturation at 95 °C for 5 s followed by annealing and extension at 60 °C for 30 s.

Table 1. Primer sequences for RT-PCR.

Target gene	Primer sequences (5′-3′)	
	Forward sequences	Reverse sequences
mIL-6	AAGAGACTTCCATCCAGTTGGC	CACTCCTTCTGTGACTCCAGC
Luciferase	AGAACTGCCTGCGTGAGATT	GGTGTTGGAGCAAGATGGAT
TNF-α	CAGCCGATGGGTTGTACCTT	CCGGACTCCGCAAAGTCTAA
IL-1β	ATCTGGGATCCTCTCCAGCC	CTGGAAGGTCCACGGGAAAG
iNOS	ATGACTCCCAGCACAAAGGG	ACGCTGAGTACCTCATTGGC
Iba-1	TCTGAGGAGCTATGAGCC	TGCTGTCATTAGAAGGTCC
GAPDH	ACTCCACTCACGGCAAATTC	CCCTGTTGCTGTAGCCGTAT

Table 2. Primer sequences for real-time PCR.

Target gene	Primer sequences (5′-3′)	
	Forward sequences	Reverse sequences
mIL-6	CTGCAAGAGACTTCCATCCAG	AGTGGTATAGACAGGTCTGTTGG
Luciferase	ACGATTTTGTGCCAGAGTCC	AGAATCTCACGCAGGCAGTT
TNF-α	AAGTCAACCTCCTCTCTGCC	CCGGACTCCGCAAAGTCTAA
IL-1β	TGTCTGAAGCAGCTATGGC	TGTTGATGTGCTGCTGCG
iNOS	ATGACTCCCAGCACAAAGGG	AACAGCACTCTCTTGCGGACC
Iba-1	TCTGAGGAGCTATGAGCC	TCCATGTACTTCGTCTTGAAGGC
GAPDH	GTCGTGGAGTCTACTGGTGTCTT	GAGATGATGACCCTTTTGGC

2.12. 3D model building of *N*-glycosylated IL-6/sIL-6R/gp130 complex

Homology modeling of murine IL-6, sIL-6R and gp130 was performed using SWISS-MODEL (46) and the template was the cryo-EM structure of human IL-6/sIL-6R/gp130 hexametric complex with stoichiometry of 2:2:2 (PDB ID: 8D82) (47). Glycan Modeler tool in CHARMM-GUI (48) was used to build a 3D structural model of *N*-glycosylated murine IL-6/sIL-6R/gp130 complex. The homology model was used as a scaffold of the artificial *N*-glycosylation (GlcNAc2Man3GlcNAc2Fuc) and all the *N*-glycosylation sequons are utilized for modification (sIL6R: N32, N55 and N150; gp130: N43, N61, N83, N131, N157, N225, N388, N476 and N551). The glycan conformation was based on the CHARMM force field (49).

2.12. Statistical analysis

All data are presented as the mean ± SD obtained from at least three independent experiments. Statistics were analyzed using a one-way analysis of variance (ANOVA) with Tukey's *post hoc* test or an unpaired Student *t*-test by GraphPad Prism® 5.0 software (GraphPad Software, Inc., La Jolla, CA). A probability value of p was considered as follows: n.s. (no significance), $p > 0.05$; *$p < 0.05$; **$p < 0.01$; ***$p < 0.001$.

3. Results

3.1 Exogenous L-fucose increased the core fucosylation in brain tissues of Fut8$^{+/-}$ mice

It has been known that the Fut8$^{+/-}$ mice exhibit a reduced amount of Fut8 and consequently diminish the core fucosylation level compared to the Fut8$^{+/+}$ control mice. To investigate whether exogenous L-fucose improves the core fucosylation level in Fut8$^{+/-}$ mice, we fed the mice by oral gavage with different doses of L-fucose twice a day for two weeks, as shown in Fig. 2A. Expectedly, the expression levels of core fucosylation in brain tissues were lower in Fut8$^{+/-}$ mice than in Fut8$^{+/+}$ mice (Fig. 2B). Similarly, the expression levels of Fut8 protein were also lower in Fut8$^{+/-}$ mice (Fig. 2B). The decreased levels of core fucosylation in the Fut8$^{+/-}$ mice were significantly rescued by L-fucose administration at 12 or 36 mg/day (Fig. 2B). Consistently, the results obtained from mass spectrometry (MS) analysis also showed that the levels of major *N*-glycans containing core fucose in the hippocampus of Fut8$^{+/-}$ mice were lower than that in Fut8$^{+/+}$ mice (Fig. 2C). As anticipated, the decreased levels of core fucosylation in the hippocampus were partially rescued by exogenous L-fucose (Fig. 2C). Furthermore, HPLC separation of nucleotide sugars demonstrated that the levels of GDP-fucose increased after L-fucose administration at 12 or 36 mg/day (Fig. 2D). Surprisingly, the level of GDP-fucose was decreased in the Fut8$^{+/-}$ mice compared to it in Fut8$^{+/+}$ mice. These results demonstrate that exogenous L-fucose can increase the modification of core fucosylation in the brain tissues *in vivo*.

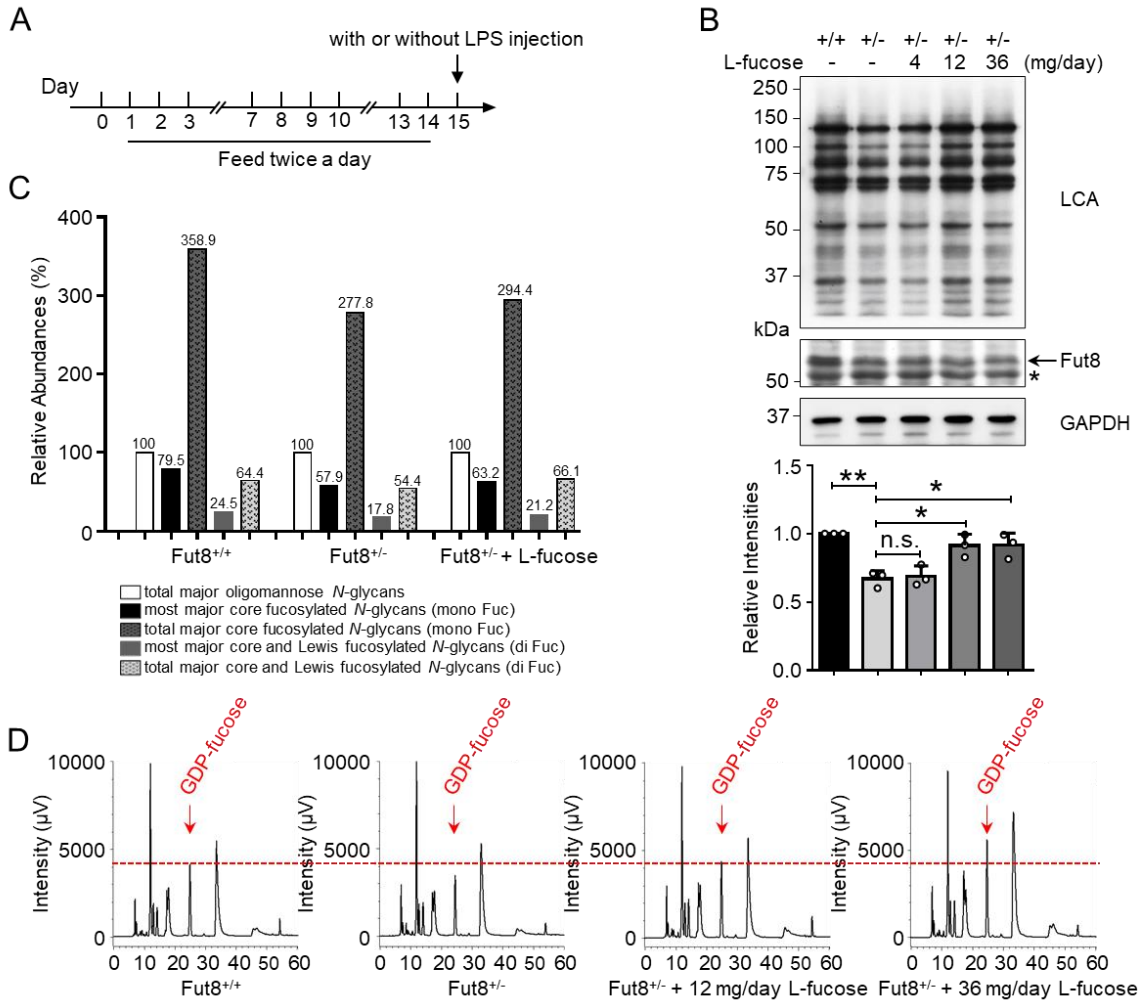

Figure 2. Effect of exogenous L-fucose on core fucosylation in the Fut8$^{+/-}$ mice. (A) Schedule of L-fucose administration using gavage twice daily before each experiment (LPS injection in the later experiments). (B) After the pretreatment described in (A), the same amounts of brain tissues were detected by LCA lectin blot and Western blotted with an anti-Fut8 antibody. The asterisk indicates the nonspecific band. GAPDH was used as a loading control. The ratio of LCA versus GAPDH of Fut8$^{+/+}$ mice treated without L-fucose was set as 1.0. Data were analyzed from all the bands of LCA lectin blot by one-way ANOVA with Tukey's multiple comparison tests and showed as the mean ± SD from three independent experiments. n.s. $p > 0.05$; *$p < 0.05$; **$p < 0.01$. (C) LC-MS analysis of *N*-glycans

obtained from the hippocampus of Fut8$^{+/+}$ mice, Fut8$^{+/-}$ mice, and Fut8$^{+/-}$ mice treated with 36 mg/day L-fucose. The intensities of major oligomannose *N*-glycans, most major core fucosylated *N*-glycans (mono Fuc), major core fucosylated *N*-glycans (mono Fuc, based on diagnostic ion in MS/MS), most major core and Lewis fucosylated *N*-glycans (di Fuc) and major core and Lewis fucosylated *N*-glycans (di Fuc, based on diagnostic ion in MS/MS) were shown in here. The relative abundances (%) calculated by setting the total intensities of major oligomannose *N*-glycans as 100%. Each data was obtained from a mixture of 3 mice. (D) The Fut8 mice were treated with equal amounts of PBS or L-fucose (12 or 36 mg/day) for two weeks. The brain tissues (50 mg) were homogenized in ice-cold 70% ethanol (500 μl). All the freeze-dried samples were subjected to ion-pair solid-phase extraction using the Envi-Carb columns. Dried nucleotide sugars were dissolved with 100 μl Milli-Q water and injected 50 μl onto the column. The GDP-fucose peak was confirmed by comparing with the retention time of GDP-fucose standard.

3.2 Exogenous L-fucose attenuated the neuroinflammation monitored by the luciferase luminescence via the WIM-6 system

Next, we evaluated the therapeutic efficacy of L-fucose against neuroinflammation via the inflammation-monitoring system, namely whole-body in vivo monitoring employing the *hIL6*-BAC-*Luc* transgenic system (WIM-6 system), which can evaluate different levels of inflammatory responses by examining the intensities of luciferase luminescence (21). The luciferase luminescence was analyzed using *in vivo* imaging system (IVIS) 4 h after the LPS treatment. The IVIS results showed that the luciferase luminescence in brain tissues was markedly increased in Fut8$^{+/-}$::*hIL6-Luc* mice than that of Fut8$^{+/+}$::*hIL6-Luc* mice (Fig. 3A, B). Very interestingly, the 14-day constant L-fucose pre-

treatment (Fig. 2A) dramatically reduced the bioluminescence (Fig. 3A, B). Subsequently, we also performed an *ex vivo* imaging to ask whether L-fucose diminishes the LPS-induced neuroinflammation. Consistent with the IVIS results, the *ex vivo* results showed a partial reduction of the *hIL6-Luc* luminescence upon L-fucose administration (Fig. 3C, D). These results indicate that L-fucose can ameliorate the neuroinflammation induced by LPS.

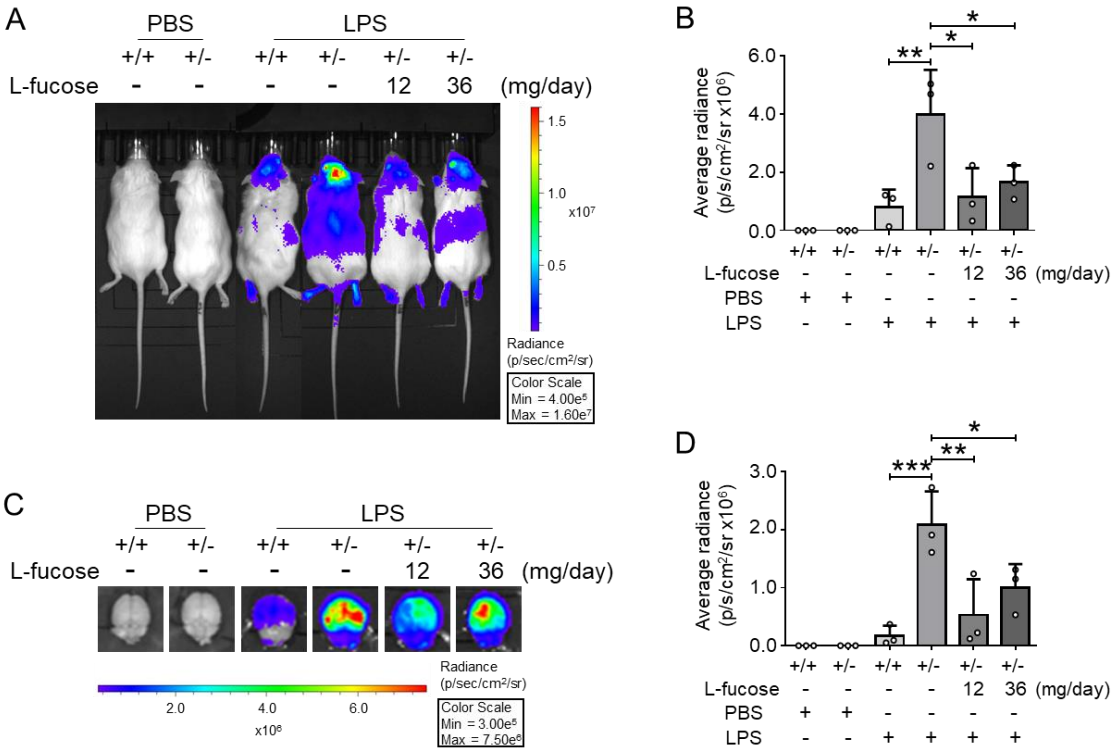

Figure 3. Monitoring the neuroinflammation by the WIM-6 system. (A) Representative images of luciferase luminescence *in vivo* 4 h after injection with or without LPS (1 mg/kg) in different groups were indicated. (B) Quantitative analysis of intensities for luciferase luminescence. All data were analyzed by one-way ANOVA test and shown as the mean ± SD from three independent experiments. The *ex vivo* imaging system also examined luciferase luminescence induced by LPS. (C) Representative images of luciferase luminescence in brain tissues. (D) Quantitative analysis of

intensities for luciferase luminescence *ex vivo*. All data were shown as the mean ± SD from three independent experiments. *$p < 0.05$; **$p < 0.01$; ***$p < 0.001$.

3.3 Effects of exogenous L-fucose on neuroinflammation induced by LPS

To further explore the efficacy of L-fucose administration on neuroinflammation, we examined expression levels of several cytokines and mediators related to inflammation. We administered the different doses (0.5, 1, 2 mg/kg) of LPS as an inflammatory stimulus to the Fut8::*hIL6-Luc* mice. RT-PCR and real-time PCR assays revealed that the LPS administration induced the IL-6 and luciferase mRNA expression dose-dependently in the $Fut8^{+/-}$ and $Fut8^{+/+}$ mice (Fig. 4A, B, C). The induced IL-6 and luciferase mRNA expression were significantly higher in the $Fut8^{+/-}$ mice than in the $Fut8^{+/+}$ mice (Fig. 4A, B, C). Of note, the basal mRNA expression of IL-6 and luciferase in the absence of the LPS stimulus was higher in the $Fut8^{+/-}$ mice than in the $Fut8^{+/+}$ mice (Fig. 4A, B, C). This result is consistent with the previous observation that $Fut8^{-/-}$ mice showed a spontaneous increase in microglial activation *in vivo* (36). In the subsequent experiments, we selected the dose at 1 mg/kg of LPS as an inducer of the neuroinflammatory model since both 1 and 2 mg/kg of LPS induced significantly different levels of IL-6 and luciferase mRNA between $Fut8^{+/-}$ and $Fut8^{+/+}$ mice.

Since exogenous L-fucose rescued the core fucosylation level and neuroinflammation in the cerebral tissues of $Fut8^{+/-}$ mice, as described above, we examined whether L-fucose administration could alleviate the inflammatory responses induced by LPS. Consistent with the IVIS results, the RT-PCR and real-time PCR results showed that the induction of IL-6 and luciferase expression by LPS were much higher in the $Fut8^{+/-}$ mice than in the $Fut8^{+/+}$ mice. The induction was significantly suppressed by L-fucose administration (Fig. 4D, E, F). Given that LPS injection may also increase pro-

inflammatory markers, we further assessed mRNA expression levels of TNF-α, IL-1β, and inducible nitric oxide synthase (iNOS) in the brain tissues. Again, the results showed that the expression levels of these pro-inflammatory cytokines were higher in the Fut8$^{+/-}$ mice than in the Fut8$^{+/+}$ mice. The induction by LPS was significantly suppressed in a L-fucose dose-dependent manner (Fig. 4G, H). These results demonstrate that a lower core fucosylation leads to enhanced neuroinflammatory status and higher sensitivity to inflammatory stimulators, which can be corrected by exogenous L-fucose administration.

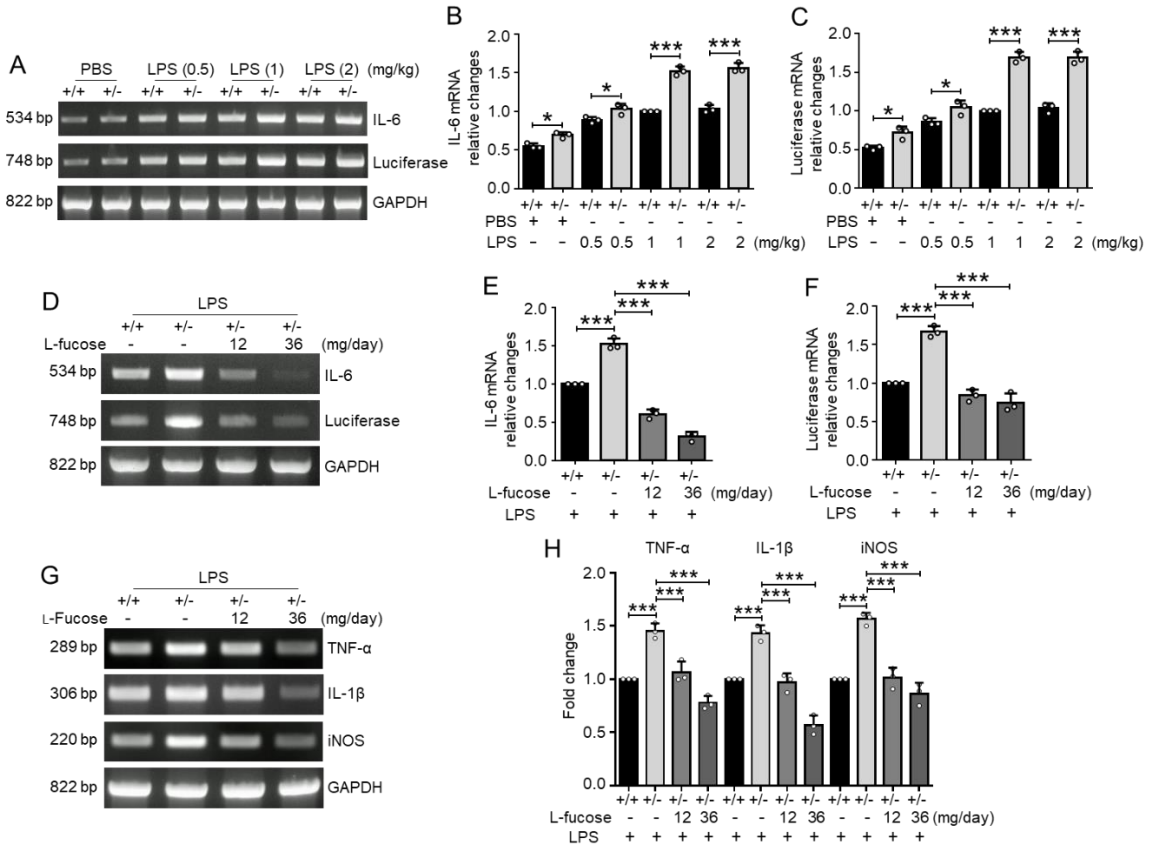

Figure 4. Alteration of inflammatory cytokines induced by LPS. The Fut8::*hIL6-Luc* mice were treated with equal amounts of PBS or LPS at indicated concentrations via intraperitoneal injection. Post 4 h after intraperitoneal injection, RT-PCR (A) and real-time PCR (B, C) detected the mRNA levels of

IL-6 and luciferase in the brain tissues. The ratio of IL-6 or luciferase versus GAPDH of Fut8$^{+/+}$::*hIL6-Luc* mice injected with 1 mg/kg LPS was set as 1.0. Values were shown as the mean ± SD from three independent experiments (one-way ANOVA test). *$p < 0.05$; ***$p < 0.001$. (D-H) The Fut8::*hIL6-Luc* mice were treated with equal amounts of PBS or L-fucose (12 or 36 mg/day) for two weeks and then intraperitoneally injected with LPS on the 15th day. Post 4 h after intraperitoneal injection, RT-PCR (D, G) and real-time PCR (E, F, H) detected the levels of inflammation factors, including IL-6 and luciferase, TNF-α, IL-1β, and iNOS in the brain tissues. GAPDH was used as an internal control. Each value was normalized to that of the GAPDH. The value of Fut8$^{+/+}$::*hIL6-Luc* mice treated without L-fucose was set as 1.0. All data were shown as the mean ± SD from three independent experiments. ***$p < 0.001$.

3.4 L-Fucose inhibited microglia activation induced by LPS in the dentate gyrus (DG)

Microglia, which account for approximately 10% of brain cells, play a pivotal role in active immune defense (50,51). Upon pathogen invasion or inflammatory stimuli, microglia transit to an activated state and generate inflammatory mediators to participate in the immune response and debris clearance (50). Nevertheless, if the stimulation exists persistently, the activated microglial cells would cause irreparable CNS injury and neuroinflammation-associated psychiatric disorders (20,50,52). One aspect of DG physiology is that it can generate new neurons throughout life (53); meanwhile, aberrant microglial activation in the DG can impair neurogenesis and cell survival (54) and lead to depression-like neurological symptoms (51,55). Therefore, suppressing microglial overactivation can be a potential strategy for preventing psychiatric diseases. Given these, we examined the glial cell activation status by detecting Iba-1, a microglia marker, in the hippocampus regions. Furthermore, the

immunostaining with anti-Iba-1 antibody showed a significant difference between Fut8$^{+/-}$ and Fut8$^{+/+}$ mice under normal conditions without LPS treatment, i.e., more Iba-1-positive cells in the Fut8$^{+/-}$ mice (Fig. 5A, B). On the other hand, after treatment with LPS, the increase in Iba-1-positive cells was more significant in the Fut8$^{+/-}$ mice than in the Fut8$^{+/+}$ mice. These enhanced staining and activation were dramatically rescued by exogenous L-fucose (Fig. 5A, B). Consistently, the RT-PCR and real-time PCR results also confirmed that the expression levels of Iba-1 were higher in Fut8$^{+/-}$ mice than in the Fut8$^{+/+}$ mice, which were suppressed by L-fucose (Fig. 5C, D). These results further suggest that core fucosylation is crucial for maintaining normal microglial status and that L-fucose supplementation can alleviate the aberrantly activated microglia.

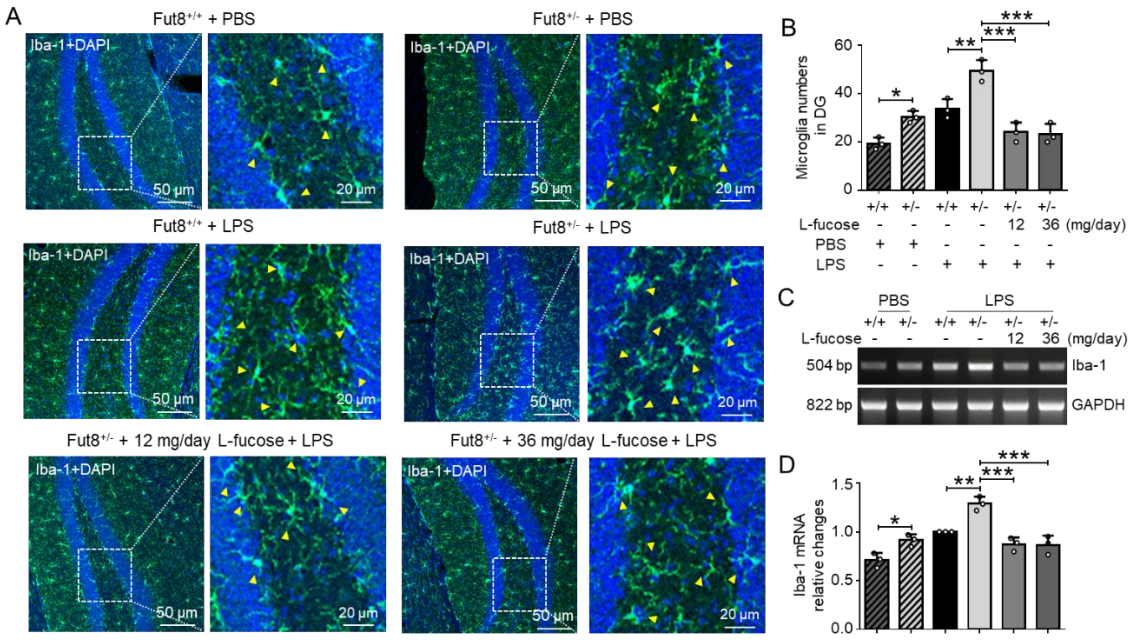

Figure 5. The overactivation of microglia induced by LPS was inhibited after L-fucose pretreatment. The Fut8::*hIL6-Luc* mice were treated with equal amounts of PBS or L-fucose twice a day for two weeks and then intraperitoneally injected with PBS or LPS for 4 h on the 15th day, as described in Fig. 2A. (A) Representative immunostaining images with anti-Iba1 antibody and DAPI in

the DG of brain tissues. Arrows indicate the activated microglia. (B) Quantitative analysis of the activated microglia. All data were shown as the mean ± SD from three independent experiments (one-way ANOVA test). *$p < 0.05$; **$p < 0.01$; ***$p < 0.001$. The expression levels of Iba-1 mRNA in the DG of brain tissues were further detected by RT-PCR (C) and real-time PCR (D). The ratio of Iba-1 versus GAPDH of Fut8$^{+/+}$::*hIL6-Luc* mice treated without L-fucose and injected with LPS was set as 1.0. All data for the quantitative analysis of the changes were shown as the mean ± SD from three independent experiments. *$p < 0.05$; **$p < 0.01$; ***$p < 0.001$.

3.5 Fut8 deletion enhanced the association of gp130 with sIL-6R and decreased the effects of L-fucose on IL-6 expression

It has been known that the pro-inflammatory property of IL-6 is mediated predominantly through the trans-signaling (27,56). In the trans-signaling pathway, IL-6 binds to the sIL-6R, forming the IL-6/sIL-6R complex, which interacts with gp130. A series of previous studies have demonstrated that core fucosylation can either positively or negatively regulate the function of the cell surface receptors. For example, core fucosylation of EGFR is required for its higher affinity with EGF ligand to upregulate downstream signaling (31), and core fucosylation on folate receptor α (FOLR1) strengthens the uptake capacity of folate (57). Conversely, the core fucosylation negatively regulates some receptors and their downstream signaling, such as AMPARs and activin receptor (32,58), as well as FcγRIII receptor (59). Considering gp130 is the most critical co-receptor for IL-6, which can mediate the downstream JAK/STAT signaling pathway (27,28), we hypothesized that the core fucosylation might regulate the complex formation between sIL-6R and gp130. Here, we used the CRISPR/Cas9 system to establish the Fut8 knockout (KO) BV-2 cell line, which was confirmed by genomic sequence

analysis. The analysis revealed a 2-base (GG) deletion in allele 1, one mutation (A was replaced by T in the red) in allele 2, and one insertion mutation (T inserted between T and G) compared to the Fut8 wide-type (WT) cells (Fig. 6A). Furthermore, the results from LCA lectin blotting and Western blot using anti-Fut8 antibody confirmed the successful deletion of the Fut8 gene (Fig. 6B). The core fucosylation of gp130 was abolished in the Fut8-KO cells (Fig. 6C). Subsequently, we validated the complex formation between sIL-6R and gp130 through co-immunoprecipitation experiments. These experiments demonstrated that a significant increase in the association between gp130 and sIL-6R in the Fut8-KO cells compared with that in the WT cells (Fig. 6D). Additionally, we validated the "feed-forward" mechanism using the BV-2 cell line. The LCA lectin results showed that the levels of core fucosylation were increased after L-fucose pre-treatment at different doses (Fig. 6E), in which the dose at 5 μM shows sufficient effect on the increase. The real-time PCR assay showed that the expression levels of IL-6 were increased in the Fut8-KO cells, compared with that in the WT cells. Interestingly, the induction of IL-6 was suppressed by the L-fucose supplementation in the WT cells, whereas the enhanced expression levels of IL-6 in the Fut8-KO cells could not be suppressed by the L-fucose (Fig. 6F). These findings strongly suggest the notion that core fucosylation negatively regulates the complex formation between gp130 and sIL-6R.

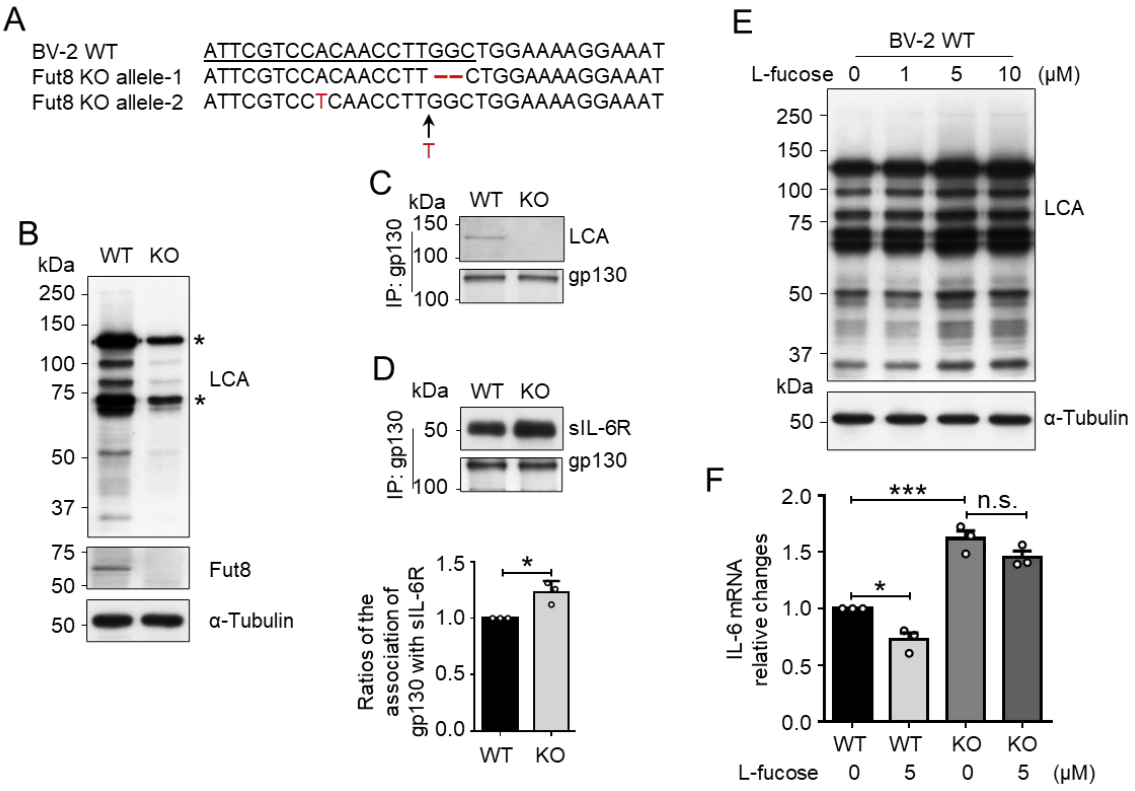

Figure 6. Fut8 negatively regulated the interaction between gp130 and sIL-6R. (A) The generation of the Fut8-KO cell line was described in the Experimental procedures and confirmed via genomic sequence analysis. (B) The validation of Fut8-KO was performed using lectin blotting with LCA and Western blotting using indicated antibodies. Asterisks indicate nonspecific staining. (C) Equal amounts of cell proteins were immunoprecipitated using Ab Capcher with an anti-gp130 antibody. The immunoprecipitated samples were subjected to lectin blotting using LCA lectin. (D) Post 4 h after LPS (1000 ng/ml) pretreatment, equal amounts of cell lysates were immunoprecipitated with an anti-gp130 antibody. Then the immunoprecipitants were Western blotted with the indicated antibodies. Data were quantified by Image J software and were shown as the mean ± SD from three independent experiments. The ratio of sIL-6R versus gp130 of WT cells was set as 1.0. *$p < 0.05$ (unpaired Student *t*-test). (E) The WT cells were cultured with L-fucose for 24 h at the indicated concentrations. Equal amounts of

cell lysates were detected by LCA lectin, and α-Tubulin was used as a loading control. (F) The cells were pretreated with or without L-fucose at 5 μM for 24 h and subsequently stimulated with LPS for 4 h. The mRNA expression levels of IL-6 were detected by real-time PCR. GAPDH was used as an internal control. Each value was normalized to that of the GAPDH. The value of WT cells treated without L-fucose was set as 1.0. Data represent the mean ± SD from three independent experiments. n.s. $p > 0.05$; *$p < 0.05$; ***$p < 0.001$. (one-way ANOVA test).

To gain structural insights on the core fucosylation on gp130, we built a 3D structural model of *N*-glycosylated IL-6/sIL-6R/gp130 complex based on the cryo-EM structure of human IL-6/sIL-6R/gp130 complex (Fig. 7) (47). Gp130 is heavily glycosylated and especially *N*-glycans on N43, N61, N83, N131, and N157 are clustered in close proximity with the other gp130 and IL-6 molecules. Furthermore, four *N*-glycans (N131 and N225 on gp130) occupy the interior space between two gp130 molecules. It is possible that core fucosylation modulates the relative orientation of the attached *N*-glycans with respect to the polypeptide and then modulates the protein-protein interactions. Further analysis is required in the future for a better understanding of the core fucosylation on gp130, such as kinetic interaction study.

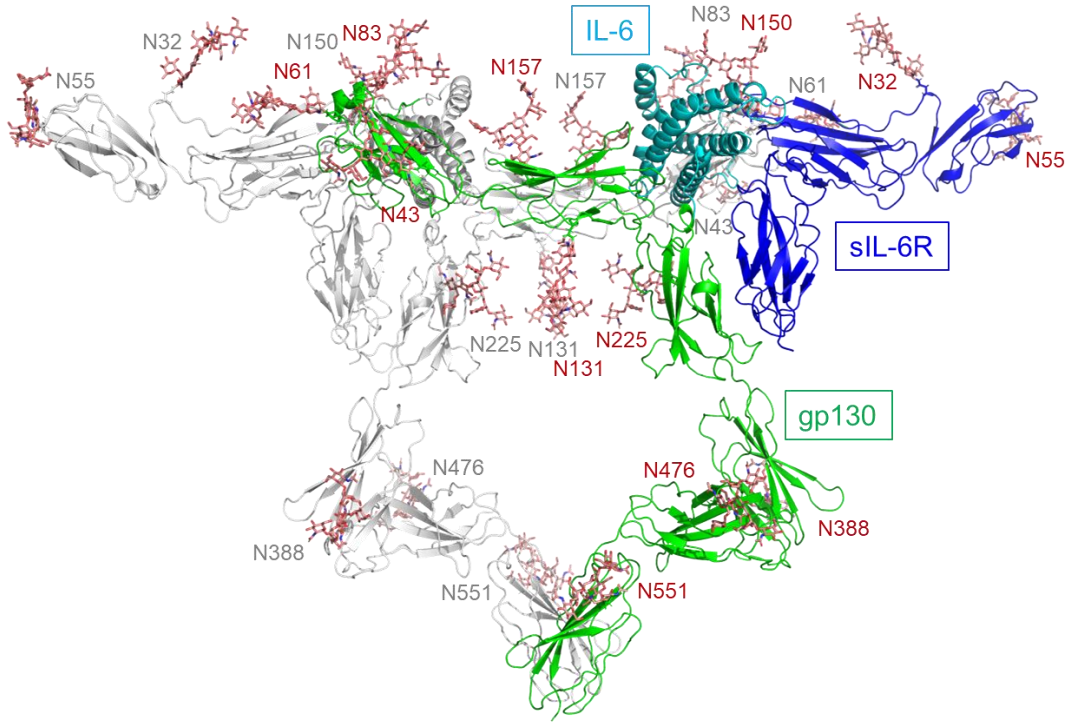

Figure 7. A 3D structural model of N-glycosylated IL-6/sIL-6R/gp130 complex. 3D structural model of *N*-glycosylated IL-6/sIL-6R/gp130 complex based on SWISS-MODEL homology modeling using the coordinates of human IL-6/sIL-6R/gp130 complex (PDB ID: 8D82) and Glycan modeler tool in CHARMM-GUI. GlcNAc2Man3GlcNAc2Fuc structure was modeled onto all potential *N*-glycosylation sites. For clarity, half of the complex model is colored: IL-6 is shown in cyan, sIL-6R in blue and gp130 in green with ribbon representation. *N*-Glycans are shown in brown with stick representation. The other half of the complex is shown in gray with ribbon representation. This figure was prepared using the PyMOL software.

3.6 Effects of exogenous L-fucose on the gp130/JAK2/Akt/STAT3 signaling

After sIL-6R complex interacts with gp130, it can lead to the activation of receptor-bound JAK2 and following phosphorylation of phosphoinositide 3-kinase (PI3K)/protein kinase B (Akt) and STAT3

(60,61). Given these, we examined the phosphorylation levels of JAK2, Akt, and STAT3. Western blot showed that the phosphorylation levels of JAK2 (Fig. 8A), Akt (Fig. 8B), and STAT3 (Fig. 8C) were all increased in the cerebral tissues of Fut8$^{+/-}$ mice, compared with that in the Fut8$^{+/+}$ mice under either normal condition or LPS treatment. Importantly, L-fucose administration significantly suppressed these increases in the phosphorylation levels (Fig. 8A, B, C). The co-immunoprecipitation results revealed an elevated association between gp130 and sIL-6R and a reduction in core fucosylation of gp130 in the Fut8$^{+/-}$::*hIL6-Luc* mice when compared with the Fut8$^{+/+}$::*hIL6-Luc* mice. Importantly, these effects were ameliorated by exogenous L-fucose (Fig. 8D). These results reveal that core fucosylation is closely involved in the pathogenesis of neuroinflammation, which may be mediated by the gp130/JAK2/Akt/STAT3 signaling pathway.

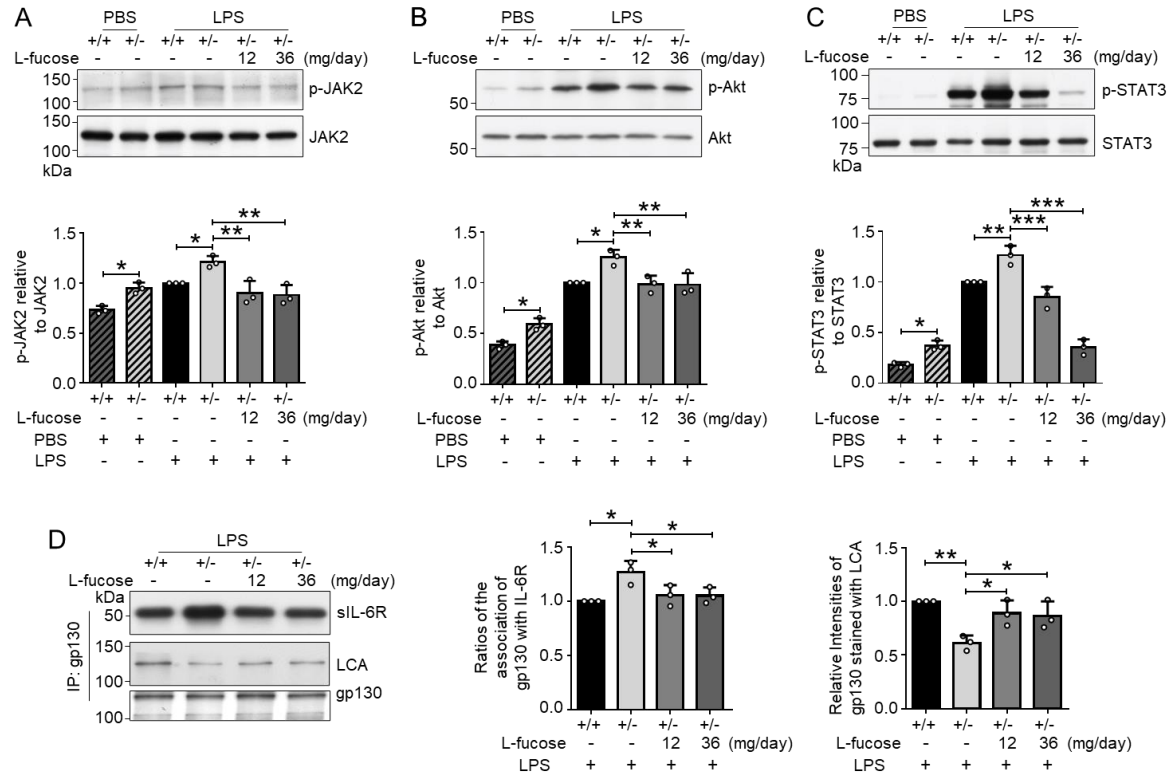

Figure 8. Effects of core fucosylation on intracellular signaling. The brain tissues were obtained from the pretreated Fut8::*hIL6-Luc* mice as described in Fig. 2A. The expression levels of phosphor-JAK2 (p-JAK2) and JAK2 (A), phosphor-Akt (p-Akt) and Akt (B), phosphor-STAT3 (p-STAT3) and STAT3 (C) were examined by Western blotting with the indicated antibodies. Data were quantified by Image J software. The ratios of p-JAK2 versus JAK2, p-Akt versus Akt or p-STAT3 versus STAT3 of Fut8$^{+/+}$::*h*IL6-*Luc* mice treated without L-fucose and injected with LPS were set as 1.0. Data were shown as the mean ± SD from three independent experiments. *$p < 0.05$; **$p < 0.01$; ***$p < 0.001$ (one-way ANOVA test). (D) Equal amounts of tissue proteins were immunoprecipitated with Ab Capcher combined with anti-gp130 antibody, and the immunoprecipitates were lectin blotted with LCA lectin or Western blotted with anti-IL-6R and anti-gp130 antibodies. Data were quantified by Image J software. The ratio of sIL-6R or LCA versus gp130 of Fut8$^{+/+}$::*hIL6-Luc* mice treated without L-fucose was set as 1.0. All data were shown as the mean ± SD from three independent experiments. *$p < 0.05$; **$p < 0.01$ (one-way ANOVA test).

3.7 Effects of L-fucose on neuroinflammation in Fut8$^{+/+}$ mice

As described above, exogenous L-fucose exerted an anti-neuroinflammatory effect in the Fut8$^{+/-}$ mice. Given this, we next asked whether L-fucose also exerts an inhibitory effect on the neuroinflammation in the Fut8$^{+/+}$ mice. The LCA lectin blot result showed that the core fucosylation was increased after L-fucose administration, even in the Fut8$^{+/+}$ mice (Fig. 9A). The RT-PCR and real-time PCR results showed that L-fucose treatment also alleviated the increased mRNA expression levels of IL-6 and luciferase in the Fut8$^{+/+}$::*hIL6-Luc* mice stimulated with the LPS (Fig. 9B, C, D). Consistent with the data obtained from the Fut8$^{+/-}$::*hIL6-Luc* mice, the phosphorylation levels of JAK2, Akt, and

STAT3 upon LPS were significantly suppressed by the pre-treatment with L-fucose (Fig. 9E, F, G). These results strongly suggest that L-fucose generally exerts an anti-neuroinflammatory effect regardless of the Fut8 genotypes.

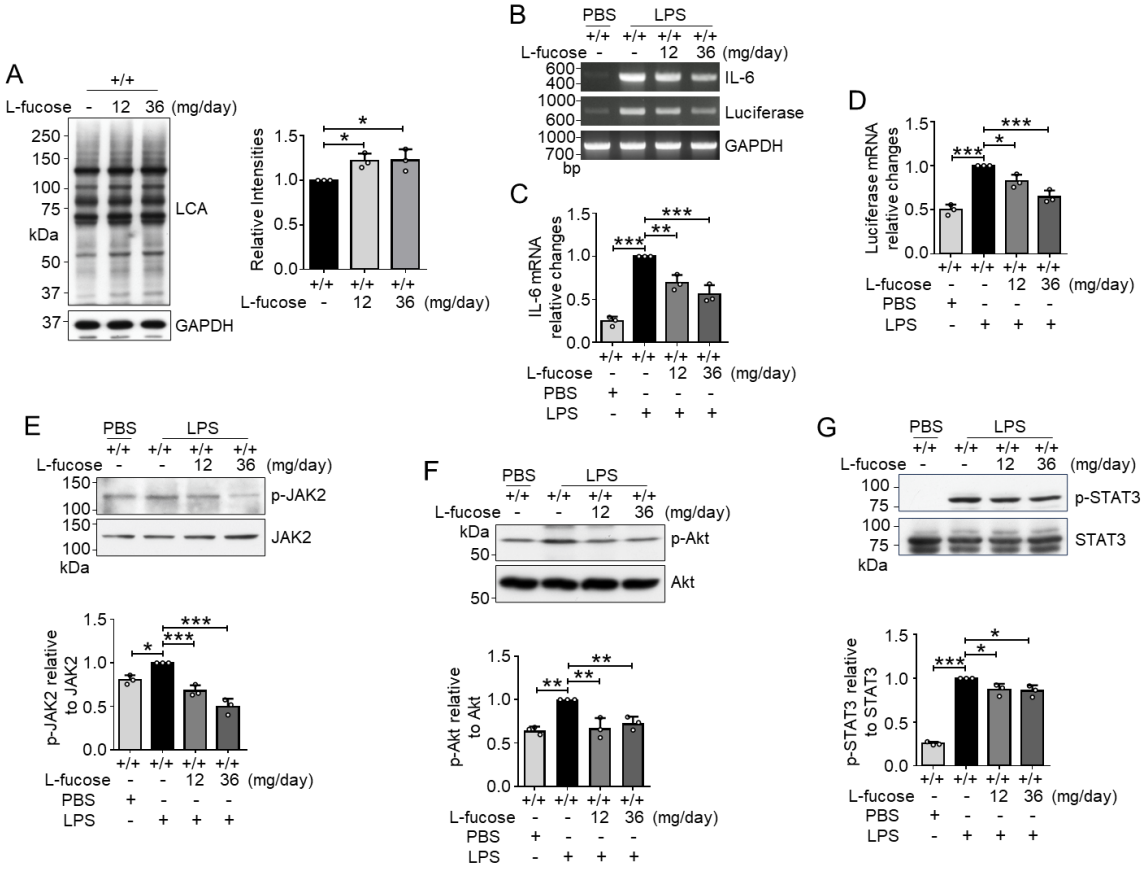

Figure 9. Effects of L-fucose on fucosylation and signaling pathway in Fut8$^{+/+}$ mice. (A) The brain tissues were obtained from the pretreated Fut8$^{+/+}$ mice as described in Fig. 2A. The core fucosylation levels were detected by lectin blot, evidenced by LCA lectin. The quantitative data were analyzed from all the bands by one-way ANOVA test and shown as the mean ± SD from three independent experiments. The ratio of LCA versus GAPDH of Fut8$^{+/+}$ mice treated without L-fucose was set as 1.0. *$p < 0.05$. The brain tissues were obtained from the pretreated Fut8$^{+/+}$::*hIL6-Luc* mice as outlined in Fig. 2A. Post 4 h after intraperitoneal injection, the mRNA levels of IL-6 and luciferase were detected

by RT-PCR (B) and real-time PCR (C, D). The quantitative data were calculated by one-way ANOVA test and shown as the mean ± SD from three independent experiments. GAPDH was used as an internal control. The value of IL-6 or luciferase versus GAPDH of Fut8$^{+/+}$::*hIL6-Luc* mice treated without L-fucose and injected with LPS was set as 1.0. *$p < 0.05$; **$p < 0.01$; ***$p < 0.001$. (E-G) Western blot examined the expression of p-JAK2 and JAK2 (E), p-Akt and Akt (F), and p-STAT3 and STAT3 (G). The ratios of p-JAK2 against JAK2, p-Akt against Akt or p-STAT3 against STAT3 of Fut8$^{+/+}$::*h*IL6-*Luc* mice treated without L-fucose and injected with LPS were set as 1.0. Data were shown as the mean ± SD from three independent experiments. *$p < 0.05$; **$p < 0.01$; ***$p < 0.001$ (one-way ANOVA test).

4. Discussion

The present study demonstrated that L-fucose exerts therapeutic efficacy against LPS-induced neuroinflammation in the Fut8$^{+/-}$ mice. We concluded that core fucosylation plays a critical role in anti-neuroinflammation, and the higher neuroinflammatory responses in the Fut8$^{+/-}$ mice are attenuated by the administration of the exogenous L-fucose. As a plausible molecular mechanism, we speculate that the defective core fucosylation on some critical target proteins, such as gp130, results in its conformational changes, which accelerate sIL-6R binding to the receptor, subsequently over-activating the downstream gp130/JAK2/Akt/STAT3 signaling pathway to further produce proinflammatory cytokines (Fig. 11).

N-Glycosylation is one of the major post-translational modifications of proteins, which correlates to protein structure and function, including correct protein folding, stability, maturation, and protein-protein interaction (62,63). Core fucosylation occurs exclusively on the core of *N*-glycans, which is catalyzed by Fut8 and is associated with numerous physiological and pathological processes (1,64). For instance, the elevated level of core fucosylated α-fetoprotein (AFP) is a reliable biomarker for hepatocellular carcinoma (65,66). And increments in core fucosylation of serum proteins have been related to the increased risk of metastasis in prostate cancer, which can be a valuable biomarker for the detection of the prostate cancer (67). Furthermore, lack of core fucosylation can enhance the affinity of human IgG1 binding to FcγRIIIa, which increases the ADCC and improves the efficacy of anticancer chemotherapeutics both *in vivo* and *in vitro* (59,68,69). Consistently, the lack of core fucosylation in mouse IgG2 confers a 10-fold increased affinity for binding to FcγRIV (70). Thus, core fucosylation plays a vital role in numerous physiological and pathological processes, and its dysregulation can be associated with various diseases.

Core fucosylation exerts various biological functions that vary among diverse cell types. $Fut8^{-/-}$ mice showed an emphysema-like pulmonary disorder due to an aberration in TGF-β1 receptor activation and downstream signaling pathway (9). Additionally, $Fut8^{+/-}$ mice exhibited a more significant increase in sensitivity to a cigarette smoke-induced emphysema model than $Fut8^{+/+}$ control mice (37). Consistent with these data, we found that the expression levels of IL-6 in lung tissues were significantly increased in $Fut8^{+/-}$ mice relative to the $Fut8^{+/+}$ mice. Furthermore, the treatment with exogenous L-fucose significantly suppressed the IL-6 expression (Fig. 10A, B, C). Our findings, accompanied by the previous data, strongly suggest that core fucosylation negatively regulates inflammation. However, it is not always the case. We also noticed that the expression levels of IL-6 in spleen tissues were significantly decreased in $Fut8^{+/-}$ mice compared to the $Fut8^{+/+}$ mice, and the exogenous L-fucose significantly upregulated the IL-6 expression (Fig. 10D, E, F). This observation can be supported by previous studies in which the deficiency of core fucosylation in CD14 could impair TLR4 signaling in mouse embryonic fibroblasts (71) and reduce the activation of RAW264.7 cells upon LPS stimulation (72). These outcomes suggest that the regulation of inflammation via core fucosylation may vary in different tissues. However, the precise mechanisms behind these tissue-specific variations require further investigation. We also speculate that the cause of altered inflammation may be related to gp130 expression level and function in different tissues. Several studies reported that gp130 is mainly involved in neuroinflammation and neurodegeneration in the brain (73,74) and is crucial for regulating inflammation and tissue repair in the lung (75,76). Nevertheless, it is also essential for developing, surviving, and activating immune cells in the spleen (77). It's worth noting that our previous study reported that lack of core fucose could induce a schizophrenia-like abnormal behavior (10,32), which is possibly due to the neuroinflammation in the CNS and immune dysfunction

(34,35,78). The deficiency of core fucosylation can upregulate the sensitivity of microglia and astrocytes to inflammatory stimuli and continuously regulate the neuroinflammation (36). Consistently, this study found lower core fucosylation leads to higher sensitivity to inflammatory stimulators and induces severe neuroinflammatory status in Fut8$^{+/-}$ mice, which exogenous L-fucose could attenuate. Thus, core fucosylation may play a critical role in regulating neuroinflammation in the brain.

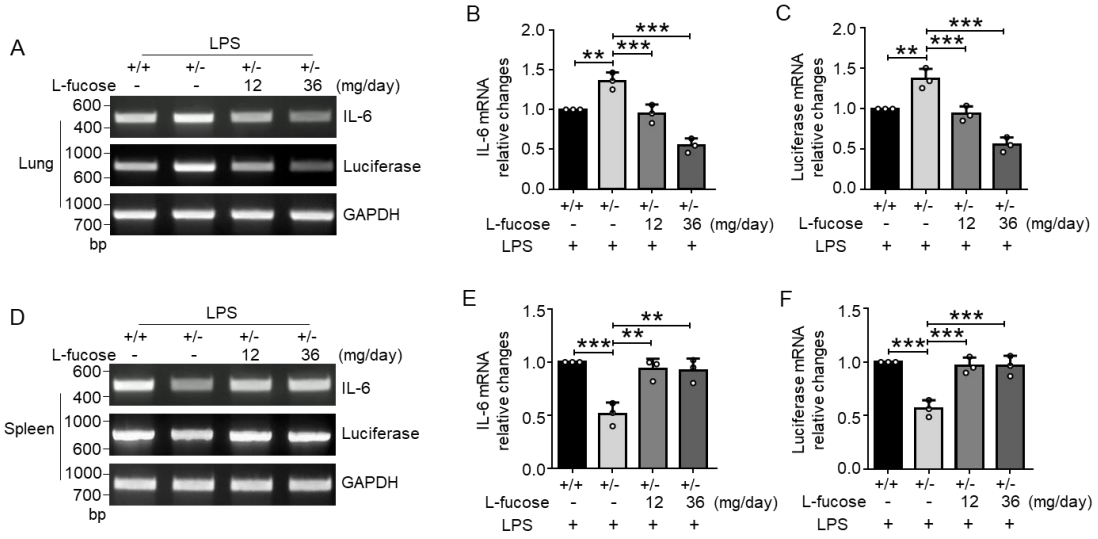

Figure 10. Schematic diagram of the proposed molecular mechanism for neuroinflammation regulated by core fucosylation. Alteration of IL-6 and luciferase induced by LPS in the lung and spleen tissues. The Fut8::*hIL6-Luc* mice were treated with equal amounts of PBS or L-fucose (12 or 36 mg/day) for two weeks and then intraperitoneally injected with LPS on the 15th day. Post 4 h after intraperitoneal injection, RT-PCR (A, D) and real-time PCR (B, C, E, F) detected the levels of IL-6 and luciferase in the lung (A-C) and spleen tissues (D-F). All data were shown as the mean ± SD from three independent experiments. GAPDH was used as an internal control. Each value was normalized to that of the GAPDH. The value of Fut8$^{+/+}$::*hIL6-Luc* mice treated without L-fucose was set as 1.0. $^{**}p < 0.01$; $^{***}p < 0.001$.

Neuroinflammation refers to the innate immune response that takes place in the brain or spinal cord, which is associated with several neurodegenerative diseases, including Parkinson's disease, Alzheimer's disease, multiple sclerosis, major depressive disorder, and amyotrophic lateral sclerosis (50,79). Microglia, the principal players in neuroinflammation, can secrete pro-inflammatory cytokines when activated, triggering immune responses and recruiting other immune cells to the site of injury or damage. It has been determined that overactivated microglia can generate a cohort of pro-inflammatory mediators, which may subsequently diminish neuronal plasticity, impair memory, and is generally considered a significant contributor to the development and progression of neurodegenerative disorders (52,80). This study found that two weeks of L-fucose administration can significantly decrease the expression of pro-inflammatory cytokines and microglial activation triggered by LPS, which could be a new strategy for treating neurodegenerative disorders.

Furthermore, free L-fucose through the metabolism pathway of the GDP-fucose (Fig. 1) can be utilized by fucosyltransferases, which plays a vital role in immune cell development, including macrophage polarization and function regulation (7). Our previous studies found that 2-fluoro-L-fucose (2FF), an inhibitor of fucosylation, could block cellular fucosylation in primary astrocytes (36) and two pancreatic adenocarcinoma cell lines, PANC-1 and MIA PaCa-2 cells in quite different doses (13), which indicates that the salvage pathway may differently affect on cellular fucosylation among cell lines or cell types. Interestingly, research by Freeze's group reported that Fut8 could preferentially utilize the GDP-fucose originating from the exogenous fucose, while the GDP-fucose deriving from endogenous fucose was used by other fucosyltransferases to modify *N*-glycan antennae (81), which may partly explain our finding here to show that exogenous L-fucose could increase the core fucosylation downregulated in $Fut8^{+/-}$ mice. Furthermore, these results are consistent with previous

research, which demonstrated that oral L-fucose supplementation rescued the intracellular fucosylation. It remains unclear whether core fucosylation increased, and markedly improved the neurological phenotype as well as the growth in one individual with biallelic GDP-L-fucose synthase (GFUS) variants (4). In addition, recently, it was reported that L-fucose was an effective agent for harmlessly enhancing intratumoral immune cells (itICs) and immunotherapy efficacy in melanoma (82). Moreover, it is worth noting that L-fucose has been demonstrated as a generally safe and well-tolerated therapeutic agent in patients with leukocyte adhesion deficiency II, also known as SLC35C1-CDG (83,84). Furthermore, fucoidan, a form of sulfated L-fucose polymers, has multiple biological and pharmacological activities, such as anti-cancer, anti-proliferation, anti-oxidation, etc. (85-87). It has already been investigated for its potential use as a dietary supplement or synergistic anti-cancer agent in combination with chemotherapeutic drugs (88-90). However, the oral bioavailability of fucoidan could be low due to its highly polar nature and molecular weight (91,92). Based on the observation that L-fucose enhanced the core fucosylation to exert an anti-neuroinflammatory effect both in $Fut8^{+/+}$ and $Fut8^{+/-}$ mice in the present study, we speculate that the effects of fucoidan on multiple cancers may be related to the anti-inflammatory effect of its monomer, L-fucose, to a certain extent.

It is well-known that the neuroinflammatory responses mediated by microglia can be regulated by many signaling molecules in the proinflammatory signaling pathway, such as JAK2/STAT3 (93,94). It can be activated by several cytokines and growth factors, such as IL-6 and erythropoietin (EPO) (27,95). In trans IL-6 signaling, IL-6 binds to the sIL-6R in circulation, then interacts with gp130, which has 9 potential *N*-glycosylation sites (96), leading to the activation of JAK2/Akt/STAT3 signaling pathway and subsequent generation of pro-inflammatory cytokines and chemokines. *N*-Glycosylation is crucial for gp130 stability, and the proteasomal degradation pathway can degrade unglycosylated gp130 before

reaching the cell surface (97). The present study showed that core fucosylation of gp130 plays an essential role in the regulation of neuroinflammation via the gp130/JAK2/Akt/STAT3 signaling pathway (Fig. 11). Aberrant activation of the JAK2/Akt/STAT3 pathway can contribute to the development of various inflammatory diseases (98), which can be suppressed by the supplement of L-fucose (Fig. 8).

The core fucosylation is highly expressed in the brain tissues, as evidenced by MS analysis (Fig. 2C). There are 79.5% most major core fucosylated *N*-glycans that containing mono fucose in $Fut8^{+/+}$ mice, whiles 57.9% in the $Fut8^{+/-}$ mice. The treatment with L-fucose could upregulate the core fucosylation from 57.9% to 63.2% in the brain of $Fut8^{+/-}$ mice (Fig. 2C). Although the increase in total core fucosylation by L-fucose was slight, its impact on neuroinflammation was significant. It could be explained that the exogenous L-fucose promotes core fucosylation on some important glycosylation sites and/or some target glycoproteins, such as gp130, as described above, rather than total glycoproteins. We do not exclude other plausible mechanisms for the L-fucose effects. For instance, α1,3-fucosylation of low-density lipoprotein receptor-related protein 6 (LRP6) could promote its endocytosis, resulting in the inhibition of Wnt/β-catenin signaling, which can be reversed by the exogenous L-fucose (99,100). Detailed information requires for further study. It is worth noting that the therapeutic impact of L-fucose on neuroinflammation was also observed in the $Fut8^{+/+}$ mice (Fig. 9). Taken together, these results provide a notion that exogenous L-fucose exerts an anti-inflammatory efficacy via regulating core fucosylation. Therefore, we propose that L-fucose can be helpful as an essential supplementation.

The present study demonstrates that core fucosylation negatively modulates the severity of the LPS-induced neuroinflammation and that the exogenous L-fucose efficiently attenuates the

neuroinflammation. Our findings may provide a novel concept of therapeutic L-fucose application in treating or preventing neurodegenerative diseases.

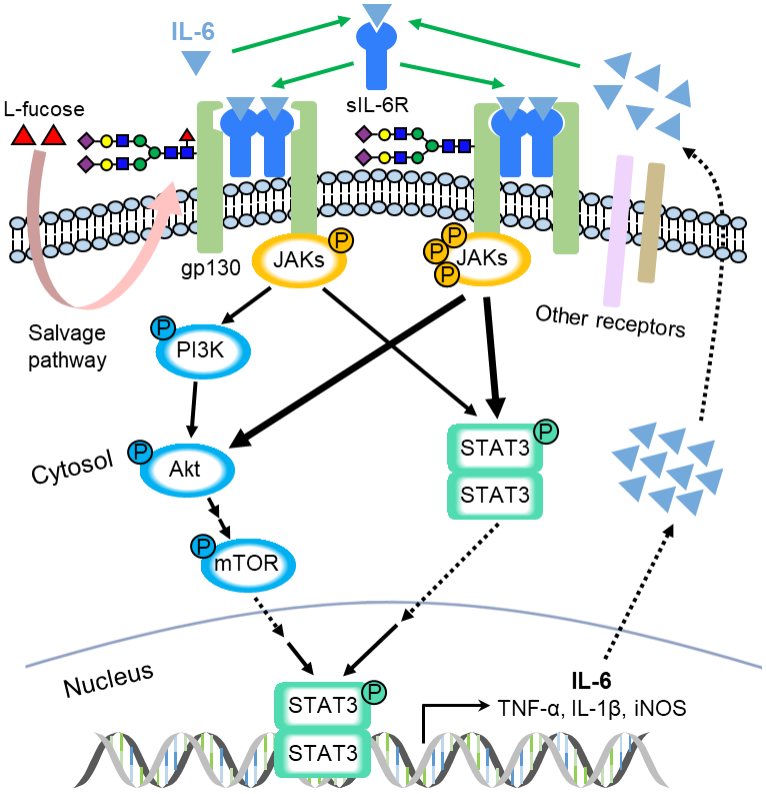

Figure 11. Schematic diagram of the proposed molecular mechanism for neuroinflammation regulated by core fucosylation. Based on our observations in the present study, core fucosylation could negatively regulate neuroinflammation induced by LPS, i.e., lower core fucosylation as shown in Fut8$^{+/-}$ mice enhanced expression of pro-inflammatory cytokines such as IL-6, TNF-α, IL-1β, and iNOS, and microglial activation to induce neuroinflammation, which could be significantly suppressed by increasing core fucosylation using exogenous L-fucose. Considering IL-6 signaling is one of the main signaling pathways involved in neuroinflammation, and sIL-6R can bind to the co-receptor gp130 to activate downstream JAK/STAT signaling pathway (27,28), we believe that the core fucosylation on gp130 may give a significant impact both *in vitro* and *in vivo*, as observed in this study. The

molecular mechanism can be postulated that lack of core fucosylation of gp130 induces its property conformation for sIL-6R binding. A similar phenomenon has been observed in the binding of IgG1 to FcγRIIIa, which was proved by structural biology studies (101,102). Of course, we do not exclude other target glycoproteins besides gp130 since the core fucosylation is highly expressed in brain tissues and modifies many other cytokine receptors, such as TGF-β and TNF-α receptors, which may also positively and negatively regulate neuroinflammation.

5. References

1. García-García, A., Ceballos-Laita, L., Serna, S., Artschwager, R., Reichardt, N. C., Corzana, F., and Hurtado-Guerrero, R. (2020) Structural basis for substrate specificity and catalysis of α1,6-fucosyltransferase. *Nat. Commun.* **11**, 973
2. Tu, Z., Lin, Y. N., and Lin, C. H. (2013) Development of fucosyltransferase and fucosidase inhibitors. *Chem. Soc. Rev.* **42**, 4459-4475
3. Adhikari, E., Liu, Q., Burton, C., Mockabee-Macias, A., Lester, D. K., and Lau, E. (2022) L-fucose, a sugary regulator of antitumor immunity and immunotherapies. *Mol. Carcinog.* **61**, 439-453
4. Feichtinger, R. G., Hüllen, A., Koller, A., Kotzot, D., Grote, V., Rapp, E., Hofbauer, P., Brugger, K., Thiel, C., Mayr, J. A., and Wortmann, S. B. (2021) A spoonful of L-fucose-an efficient therapy for GFUS-CDG, a new glycosylation disorder. *EMBO Mol. Med.* **13**, e14332
5. Staudacher, E., Altmann, F., Wilson, I. B., and März, L. (1999) Fucose in N-glycans: from plant to man. *Biochim. Biophys. Acta.* **1473**, 216-236
6. Citkowska, A., Szekalska, M., and Winnicka, K. (2019) Possibilities of Fucoidan Utilization in the Development of Pharmaceutical Dosage Forms. *Mar. Drugs* **17**
7. Wang, Y., Huang, D., Chen, K. Y., Cui, M., Wang, W., Huang, X., Awadellah, A., Li, Q., Friedman, A., Xin, W. W., Di Martino, L., Cominelli, F., Miron, A., Chan, R., Fox, J. G., Xu, Y., Shen, X., Kalady, M. F., Markowitz, S., Maillard, I., Lowe, J. B., Xin, W., and Zhou, L. (2017) Fucosylation Deficiency in Mice Leads to Colitis and Adenocarcinoma. *Gastroenterology* **152**, 193-205.e110

8. Moriwaki, K., Noda, K., Nakagawa, T., Asahi, M., Yoshihara, H., Taniguchi, N., Hayashi, N., and Miyoshi, E. (2007) A high expression of GDP-fucose transporter in hepatocellular carcinoma is a key factor for increases in fucosylation. *Glycobiology* **17**, 1311-1320

9. Wang, X., Inoue, S., Gu, J., Miyoshi, E., Noda, K., Li, W., Mizuno-Horikawa, Y., Nakano, M., Asahi, M., Takahashi, M., Uozumi, N., Ihara, S., Lee, S. H., Ikeda, Y., Yamaguchi, Y., Aze, Y., Tomiyama, Y., Fujii, J., Suzuki, K., Kondo, A., Shapiro, S. D., Lopez-Otin, C., Kuwaki, T., Okabe, M., Honke, K., and Taniguchi, N. (2005) Dysregulation of TGF-beta1 receptor activation leads to abnormal lung development and emphysema-like phenotype in core fucose-deficient mice. *Proc. Natl. Acad. Sci. U. S. A.* **102**, 15791-15796

10. Fukuda, T., Hashimoto, H., Okayasu, N., Kameyama, A., Onogi, H., Nakagawasai, O., Nakazawa, T., Kurosawa, T., Hao, Y., Isaji, T., Tadano, T., Narimatsu, H., Taniguchi, N., and Gu, J. (2011) Alpha1,6-fucosyltransferase-deficient mice exhibit multiple behavioral abnormalities associated with a schizophrenia-like phenotype: importance of the balance between the dopamine and serotonin systems. *J. Biol. Chem.* **286**, 18434-18443

11. Wang, Y., Fukuda, T., Isaji, T., Lu, J., Im, S., Hang, Q., Gu, W., Hou, S., Ohtsubo, K., and Gu, J. (2015) Loss of α1,6-fucosyltransferase inhibits chemical-induced hepatocellular carcinoma and tumorigenesis by down-regulating several cell signaling pathways. *FASEB J.* **29**, 3217-3227

12. Chen, C. Y., Jan, Y. H., Juan, Y. H., Yang, C. J., Huang, M. S., Yu, C. J., Yang, P. C., Hsiao, M., Hsu, T. L., and Wong, C. H. (2013) Fucosyltransferase 8 as a functional regulator of nonsmall cell lung cancer. *Proc. Natl. Acad. Sci. U. S. A.* **110**, 630-635

13. Liang, C., Fukuda, T., Isaji, T., Duan, C., Song, W., Wang, Y., and Gu, J. (2021) α1,6-Fucosyltransferase contributes to cell migration and proliferation as well as to cancer stemness features in pancreatic carcinoma. *Biochim. Biophys. Acta. Gen. Subj.* **1865**, 129870

14. Larsen, M. D., de Graaf, E. L., Sonneveld, M. E., Plomp, H. R., Nouta, J., Hoepel, W., Chen, H. J., Linty, F., Visser, R., Brinkhaus, M., Šuštić, T., de Taeye, S. W., Bentlage, A. E. H., Toivonen, S., Koeleman, C. A. M., Sainio, S., Kootstra, N. A., Brouwer, P. J. M., Geyer, C. E., Derksen, N. I. L., Wolbink, G., de Winther, M., Sanders, R. W., van Gils, M. J., de Bruin, S., Vlaar, A. P. J., Rispens, T., den Dunnen, J., Zaaijer, H. L., Wuhrer, M., Ellen van der Schoot, C., and Vidarsson, G. (2021) Afucosylated IgG characterizes enveloped viral responses and correlates with COVID-19 severity. *Science* **371**

15. Sun, Y., Li, X., Wang, T., and Li, W. (2022) Core Fucosylation Regulates the Function of Pre-BCR, BCR and IgG in Humoral Immunity. *Front. Immunol.* **13**, 844427

16. Leng, F., and Edison, P. (2021) Neuroinflammation and microglial activation in Alzheimer disease: where do we go from here? *Nat. Rev. Neurol.* **17**, 157-172

17. Rebelo, A. L., Gubinelli, F., Roost, P., Jan, C., Brouillet, E., Van Camp, N., Drake, R. R., Saldova, R., and Pandit, A. (2021) Complete spatial characterisation of N-glycosylation upon striatal neuroinflammation in the rodent brain. *J. Neuroinflammation* **18**, 116

18. Gomez Perdiguero, E., Klapproth, K., Schulz, C., Busch, K., Azzoni, E., Crozet, L., Garner, H., Trouillet, C., de Bruijn, M. F., Geissmann, F., and Rodewald, H. R. (2015) Tissue-resident macrophages originate from yolk-sac-derived erythro-myeloid progenitors. *Nature* **518**, 547-551

19. Prinz, M., Jung, S., and Priller, J. (2019) Microglia Biology: One Century of Evolving Concepts. *Cell* **179**, 292-311

20. Xu, X., Hu, P., Ma, Y., Tong, L., Wang, D., Wu, Y., Chen, Z., and Huang, C. (2020) Identification of a pro-elongation effect of diallyl disulfide, a major organosulfur compound in garlic oil, on microglial process. *J. Nutr. Biochem.* **78**, 108323

21. Hayashi, M., Takai, J., Yu, L., Motohashi, H., Moriguchi, T., and Yamamoto, M. (2015) Whole-Body In Vivo Monitoring of Inflammatory Diseases Exploiting Human Interleukin 6-Luciferase Transgenic Mice. *Mol. Cell. Biol.* **35**, 3590-3601

22. Sanchis, P., Fernández-Gayol, O., Vizueta, J., Comes, G., Canal, C., Escrig, A., Molinero, A., Giralt, M., and Hidalgo, J. (2020) Microglial cell-derived interleukin-6 influences behavior and inflammatory response in the brain following traumatic brain injury. *Glia* **68**, 999-1016

23. Maimone, D., Guazzi, G. C., and Annunziata, P. (1997) IL-6 detection in multiple sclerosis brain. *J. Neurol. Sci.* **146**, 59-65

24. Sanchis, P., Fernández-Gayol, O., Comes, G., Escrig, A., Giralt, M., Palmiter, R. D., and Hidalgo, J. (2020) Interleukin-6 Derived from the Central Nervous System May Influence the Pathogenesis of Experimental Autoimmune Encephalomyelitis in a Cell-Dependent Manner. *Cells* **9**

25. Hu, J., Feng, X., Valdearcos, M., Lutrin, D., Uchida, Y., Koliwad, S. K., and Maze, M. (2018) Interleukin-6 is both necessary and sufficient to produce perioperative neurocognitive disorder in mice. *Br. J. Anaesth.* **120**, 537-545

26. Kelly, K. M., Smith, J. A., and Mezuk, B. (2021) Depression and interleukin-6 signaling: A Mendelian Randomization study. *Brain Behav. Immun.* **95**, 106-114

27. Escrig, A., Canal, C., Sanchis, P., Fernández-Gayol, O., Montilla, A., Comes, G., Molinero, A., Giralt, M., Giménez-Llort, L., Becker-Pauly, C., Rose-John, S., and Hidalgo, J. (2019) IL-6 trans-signaling in the brain influences the behavioral and physio-pathological phenotype of the Tg2576 and 3xTgAD mouse models of Alzheimer's disease. *Brain Behav. Immun.* **82**, 145-159

28. Campbell, I. L., Erta, M., Lim, S. L., Frausto, R., May, U., Rose-John, S., Scheller, J., and Hidalgo, J. (2014) Trans-signaling is a dominant mechanism for the pathogenic actions of interleukin-6 in the brain. *J. Neurosci.* **34**, 2503-2513

29. Fujii, H., Shinzaki, S., Iijima, H., Wakamatsu, K., Iwamoto, C., Sobajima, T., Kuwahara, R., Hiyama, S., Hayashi, Y., Takamatsu, S., Uozumi, N., Kamada, Y., Tsujii, M., Taniguchi, N., Takehara, T., and Miyoshi, E. (2016) Core Fucosylation on T Cells, Required for Activation of T-Cell Receptor Signaling and Induction of Colitis in Mice, Is Increased in Patients With Inflammatory Bowel Disease. *Gastroenterology* **150**, 1620-1632

30. Zhao, Y., Itoh, S., Wang, X., Isaji, T., Miyoshi, E., Kariya, Y., Miyazaki, K., Kawasaki, N., Taniguchi, N., and Gu, J. (2006) Deletion of core fucosylation on alpha3beta1 integrin down-regulates its functions. *J. Biol. Chem.* **281**, 38343-38350

31. Wang, X., Gu, J., Ihara, H., Miyoshi, E., Honke, K., and Taniguchi, N. (2006) Core fucosylation regulates epidermal growth factor receptor-mediated intracellular signaling. *J. Biol. Chem.* **281**, 2572-2577

32. Gu, W., Fukuda, T., Isaji, T., Hang, Q., Lee, H. H., Sakai, S., Morise, J., Mitoma, J., Higashi, H., Taniguchi, N., Yawo, H., Oka, S., and Gu, J. (2015) Loss of α1,6-Fucosyltransferase Decreases Hippocampal Long Term Potentiation: IMPLICATIONS FOR CORE

FUCOSYLATION IN THE REGULATION OF AMPA RECEPTOR HETEROMERIZATION AND CELLULAR SIGNALING. *J. Biol. Chem.* **290**, 17566-17575

33. Ng, B. G., Xu, G., Chandy, N., Steyermark, J., Shinde, D. N., Radtke, K., Raymond, K., Lebrilla, C. B., AlAsmari, A., Suchy, S. F., Powis, Z., Faqeih, E. A., Berry, S. A., Kronn, D. F., and Freeze, H. H. (2018) Biallelic Mutations in FUT8 Cause a Congenital Disorder of Glycosylation with Defective Fucosylation. *Am. J. Hum. Genet.* **102**, 188-195

34. Howes, O. D., and McCutcheon, R. (2017) Inflammation and the neural diathesis-stress hypothesis of schizophrenia: a reconceptualization. *Transl. Psychiatry* **7**, e1024

35. Pasternak, O., Kubicki, M., and Shenton, M. E. (2016) In vivo imaging of neuroinflammation in schizophrenia. *Schizophr. Res.* **173**, 200-212

36. Lu, X., Zhang, D., Shoji, H., Duan, C., Zhang, G., Isaji, T., Wang, Y., Fukuda, T., and Gu, J. (2019) Deficiency of α1,6-fucosyltransferase promotes neuroinflammation by increasing the sensitivity of glial cells to inflammatory mediators. *Biochim. Biophys. Acta. Gen. Subj.* **1863**, 598-608

37. Gao, C., Maeno, T., Ota, F., Ueno, M., Korekane, H., Takamatsu, S., Shirato, K., Matsumoto, A., Kobayashi, S., Yoshida, K., Kitazume, S., Ohtsubo, K., Betsuyaku, T., and Taniguchi, N. (2012) Sensitivity of heterozygous α1,6-fucosyltransferase knock-out mice to cigarette smoke-induced emphysema: implication of aberrant transforming growth factor-β signaling and matrix metalloproteinase gene expression. *J. Biol. Chem.* **287**, 16699-16708

38. Choi, S. S., Lynch, B. S., Baldwin, N., Dakoulas, E. W., Roy, S., Moore, C., Thorsrud, B. A., and Röhrig, C. H. (2015) Safety evaluation of the human-identical milk monosaccharide, l-fucose. *Regul. Toxicol. Pharmacol.* **72**, 39-48

39. Matsumura, K., Higashida, K., Ishida, H., Hata, Y., Yamamoto, K., Shigeta, M., Mizuno-Horikawa, Y., Wang, X., Miyoshi, E., Gu, J., and Taniguchi, N. (2007) Carbohydrate binding specificity of a fucose-specific lectin from Aspergillus oryzae: a novel probe for core fucose. *J. Biol. Chem.* **282**, 15700-15708

40. Wang, Y., Fukuda, T., Isaji, T., Lu, J., Gu, W., Lee, H. H., Ohkubo, Y., Kamada, Y., Taniguchi, N., Miyoshi, E., and Gu, J. (2015) Loss of α1,6-fucosyltransferase suppressed liver regeneration: implication of core fucose in the regulation of growth factor receptor-mediated cellular signaling. *Sci. Rep.* **5**, 8264

41. Harada, Y., Nakajima, K., Li, S., Suzuki, T., and Taniguchi, N. (2021) Protocol for analyzing the biosynthesis and degradation of N-glycan precursors in mammalian cells. *STAR Protoc.* **2**, 100316

42. Nakajima, K., Kitazume, S., Angata, T., Fujinawa, R., Ohtsubo, K., Miyoshi, E., and Taniguchi, N. (2010) Simultaneous determination of nucleotide sugars with ion-pair reversed-phase HPLC. *Glycobiology* **20**, 865-871

43. Skurska, E., Szulc, B., Maszczak-Seneczko, D., Wiktor, M., Wiertelak, W., Makowiecka, A., and Olczak, M. (2022) Incorporation of fucose into glycans independent of the GDP-fucose transporter SLC35C1 preferentially utilizes salvaged over de novo GDP-fucose. *J. Biol. Chem.* **298**, 102206

44. Nakano, M., Saldanha, R., Göbel, A., Kavallaris, M., and Packer, N. H. (2011) Identification of glycan structure alterations on cell membrane proteins in desoxyepothilone B resistant leukemia cells. *Mol. Cell. Proteomics* **10**, M111.009001

45. Nakano, M., Mishra, S. K., Tokoro, Y., Sato, K., Nakajima, K., Yamaguchi, Y., Taniguchi, N., and Kizuka, Y. (2019) Bisecting GlcNAc Is a General Suppressor of Terminal Modification of N-glycan. *Mol. Cell. Proteomics* **18**, 2044-2057

46. Waterhouse, A., Bertoni, M., Bienert, S., Studer, G., Tauriello, G., Gumienny, R., Heer, F. T., de Beer, T. A. P., Rempfer, C., Bordoli, L., Lepore, R., and Schwede, T. (2018) SWISS-MODEL: homology modelling of protein structures and complexes. *Nucleic Acids Res.* **46**, W296-w303

47. Zhou, Y., Stevis, P. E., Cao, J., Saotome, K., Wu, J., Glatman Zaretsky, A., Haxhinasto, S., Yancopoulos, G. D., Murphy, A. J., Sleeman, M. W., Olson, W. C., and Franklin, M. C. (2023) Structural insights into the assembly of gp130 family cytokine signaling complexes. *Sci. Adv.* **9**, eade4395

48. Park, S. J., Lee, J., Qi, Y., Kern, N. R., Lee, H. S., Jo, S., Joung, I., Joo, K., Lee, J., and Im, W. (2019) CHARMM-GUI Glycan Modeler for modeling and simulation of carbohydrates and glycoconjugates. *Glycobiology* **29**, 320-331

49. Guvench, O., Hatcher, E. R., Venable, R. M., Pastor, R. W., and Mackerell, A. D. (2009) CHARMM Additive All-Atom Force Field for Glycosidic Linkages between Hexopyranoses. *J. Chem. Theory Comput.* **5**, 2353-2370

50. Glass, C. K., Saijo, K., Winner, B., Marchetto, M. C., and Gage, F. H. (2010) Mechanisms underlying inflammation in neurodegeneration. *Cell* **140**, 918-934

51. Kreisel, T., Frank, M. G., Licht, T., Reshef, R., Ben-Menachem-Zidon, O., Baratta, M. V., Maier, S. F., and Yirmiya, R. (2014) Dynamic microglial alterations underlie stress-induced depressive-like behavior and suppressed neurogenesis. *Mol. Psychiatry* **19**, 699-709

52. Muzio, L., Viotti, A., and Martino, G. (2021) Microglia in Neuroinflammation and Neurodegeneration: From Understanding to Therapy. *Front. Neurosci.* **15**, 742065

53. Yun, S., Reynolds, R. P., Masiulis, I., and Eisch, A. J. (2016) Re-evaluating the link between neuropsychiatric disorders and dysregulated adult neurogenesis. *Nat. Med.* **22**, 1239-1247

54. Cope, E. C., and Gould, E. (2019) Adult Neurogenesis, Glia, and the Extracellular Matrix. *Cell stem cell* **24**, 690-705

55. Tong, L., Gong, Y., Wang, P., Hu, W., Wang, J., Chen, Z., Zhang, W., and Huang, C. (2017) Microglia Loss Contributes to the Development of Major Depression Induced by Different Types of Chronic Stresses. *Neurochem. Res.* **42**, 2698-2711

56. Chen, W., Yuan, H., Cao, W., Wang, T., Chen, W., Yu, H., Fu, Y., Jiang, B., Zhou, H., Guo, H., and Zhao, X. (2019) Blocking interleukin-6 trans-signaling protects against renal fibrosis by suppressing STAT3 activation. *Theranostics* **9**, 3980-3991

57. Jia, L., Li, J., Li, P., Liu, D., Li, J., Shen, J., Zhu, B., Ma, C., Zhao, T., Lan, R., Dang, L., Li, W., and Sun, S. (2021) Site-specific glycoproteomic analysis revealing increased core-fucosylation on FOLR1 enhances folate uptake capacity of HCC cells to promote EMT. *Theranostics* **11**, 6905-6921

58. Gu, W., Fukuda, T., Isaji, T., Hashimoto, H., Wang, Y., and Gu, J. (2013) α1,6-Fucosylation regulates neurite formation via the activin/phospho-Smad2 pathway in PC12 cells: the implicated dual effects of Fut8 for TGF-β/activin-mediated signaling. *FASEB J.* **27**, 3947-3958

59. Shields, R. L., Lai, J., Keck, R., O'Connell, L. Y., Hong, K., Meng, Y. G., Weikert, S. H., and Presta, L. G. (2002) Lack of fucose on human IgG1 N-linked oligosaccharide improves binding to human Fcgamma RIII and antibody-dependent cellular toxicity. *J. Biol. Chem.* **277**, 26733-26740

60. Garbers, C., Hermanns, H. M., Schaper, F., Müller-Newen, G., Grötzinger, J., Rose-John, S., and Scheller, J. (2012) Plasticity and cross-talk of interleukin 6-type cytokines. *Cytokine Growth Factor Rev.* **23**, 85-97

61. Li, Z. W., Sun, B., Gong, T., Guo, S., Zhang, J., Wang, J., Sugawara, A., Jiang, M., Yan, J., Gurary, A., Zheng, X., Gao, B., Xiao, S. Y., Chen, W., Ma, C., Farrar, C., Zhu, C., Chan, O. T. M., Xin, C., Winnicki, A., Winnicki, J., Tang, M., Park, R., Winnicki, M., Diener, K., Wang, Z., Liu, Q., Chu, C. H., Arter, Z. L., Yue, P., Alpert, L., Hui, G. S., Fei, P., Turkson, J., Yang, W., Wu, G., Tao, A., Ramos, J. W., Moisyadi, S., Holcombe, R. F., Jia, W., Birnbaumer, L., Zhou, X., and Chu, W. M. (2019) GNAI1 and GNAI3 Reduce Colitis-Associated Tumorigenesis in Mice by Blocking IL6 Signaling and Down-regulating Expression of GNAI2. *Gastroenterology* **156**, 2297-2312

62. Conroy, L. R., Hawkinson, T. R., Young, L. E. A., Gentry, M. S., and Sun, R. C. (2021) Emerging roles of N-linked glycosylation in brain physiology and disorders. *Trends Endocrinol. Metab.* **32**, 980-993

63. Schwarz, F., and Aebi, M. (2011) Mechanisms and principles of N-linked protein glycosylation. *Curr: Opin. Struct. Biol.* **21**, 576-582

64. Okeley, N. M., Alley, S. C., Anderson, M. E., Boursalian, T. E., Burke, P. J., Emmerton, K. M., Jeffrey, S. C., Klussman, K., Law, C. L., Sussman, D., Toki, B. E., Westendorf, L., Zeng, W.,

Zhang, X., Benjamin, D. R., and Senter, P. D. (2013) Development of orally active inhibitors of protein and cellular fucosylation. *Proc. Natl. Acad. Sci. U. S. A.* **110**, 5404-5409

65. Miyoshi, E., Moriwaki, K., and Nakagawa, T. (2008) Biological function of fucosylation in cancer biology. *J. Biochem.* **143**, 725-729

66. Schneider, M., Al-Shareffi, E., and Haltiwanger, R. S. (2017) Biological functions of fucose in mammals. *Glycobiology* **27**, 601-618

67. Kyselova, Z., Mechref, Y., Al Bataineh, M. M., Dobrolecki, L. E., Hickey, R. J., Vinson, J., Sweeney, C. J., and Novotny, M. V. (2007) Alterations in the serum glycome due to metastatic prostate cancer. *J. Proteome Res.* **6**, 1822-1832

68. Dekkers, G., Treffers, L., Plomp, R., Bentlage, A. E. H., de Boer, M., Koeleman, C. A. M., Lissenberg-Thunnissen, S. N., Visser, R., Brouwer, M., Mok, J. Y., Matlung, H., van den Berg, T. K., van Esch, W. J. E., Kuijpers, T. W., Wouters, D., Rispens, T., Wuhrer, M., and Vidarsson, G. (2017) Decoding the Human Immunoglobulin G-Glycan Repertoire Reveals a Spectrum of Fc-Receptor- and Complement-Mediated-Effector Activities. *Front. Immunol.* **8**, 877

69. Zeitlin, L., Pettitt, J., Scully, C., Bohorova, N., Kim, D., Pauly, M., Hiatt, A., Ngo, L., Steinkellner, H., Whaley, K. J., and Olinger, G. G. (2011) Enhanced potency of a fucose-free monoclonal antibody being developed as an Ebola virus immunoprotectant. *Proc. Natl. Acad. Sci. U. S. A.* **108**, 20690-20694

70. Nimmerjahn, F., and Ravetch, J. V. (2005) Divergent immunoglobulin g subclass activity through selective Fc receptor binding. *Science* **310**, 1510-1512

71. Iijima, J., Kobayashi, S., Kitazume, S., Kizuka, Y., Fujinawa, R., Korekane, H., Shibata, T., Saitoh, S. I., Akashi-Takamura, S., Miyake, K., Miyoshi, E., and Taniguchi, N. (2017) Core

fucose is critical for CD14-dependent Toll-like receptor 4 signaling. *Glycobiology* **27**, 1006-1015

72. Nakayama, K., Wakamatsu, K., Fujii, H., Shinzaki, S., Takamatsu, S., Kitazume, S., Kamada, Y., Takehara, T., Taniguchi, N., and Miyoshi, E. (2019) Core fucose is essential glycosylation for CD14-dependent Toll-like receptor 4 and Toll-like receptor 2 signalling in macrophages. *J. Biochem.* **165**, 227-237

73. Hu, Z., Deng, N., Liu, K., Zhou, N., Sun, Y., and Zeng, W. (2020) CNTF-STAT3-IL-6 Axis Mediates Neuroinflammatory Cascade across Schwann Cell-Neuron-Microglia. *Cell Rep.* **31**, 107657

74. Mirabella, F., Desiato, G., Mancinelli, S., Fossati, G., Rasile, M., Morini, R., Markicevic, M., Grimm, C., Amegandjin, C., Termanini, A., Peano, C., Kunderfranco, P., di Cristo, G., Zerbi, V., Menna, E., Lodato, S., Matteoli, M., and Pozzi, D. (2021) Prenatal interleukin 6 elevation increases glutamatergic synapse density and disrupts hippocampal connectivity in offspring. *Immunity* **54**, 2611-2631.e2618

75. Thompson, L. C., Holland, N. A., Snyder, R. J., Luo, B., Becak, D. P., Odom, J. T., Harrison, B. S., Brown, J. M., Gowdy, K. M., and Wingard, C. J. (2016) Pulmonary instillation of MWCNT increases lung permeability, decreases gp130 expression in the lungs, and initiates cardiovascular IL-6 transsignaling. *Am. J. Physiol. Lung Cell. Mol. Physiol.* **310**, L142-154

76. Hirani, D., Alvira, C. M., Danopoulos, S., Milla, C., Donato, M., Tian, L., Mohr, J., Dinger, K., Vohlen, C., Selle, J., S, V. K.-R., Barbarino, V., Pallasch, C., Rose-John, S., Odenthal, M., Pryhuber, G. S., Mansouri, S., Savai, R., Seeger, W., Khatri, P., Al Alam, D., Dötsch, J., and

Alejandre Alcazar, M. A. (2022) Macrophage-derived IL-6 trans-signalling as a novel target in the pathogenesis of bronchopulmonary dysplasia. *Eur. Respir. J.* **59**

77. Hunter, C. A., and Jones, S. A. (2015) IL-6 as a keystone cytokine in health and disease. *Nat. Immunol.* **16**, 448-457

78. Najjar, S., and Pearlman, D. M. (2015) Neuroinflammation and white matter pathology in schizophrenia: systematic review. *Schizophr. Res.* **161**, 102-112

79. Wang, Y., Gao, C., Gao, T., Zhao, L., Zhu, S., and Guo, L. (2021) Plasma exosomes from depression ameliorate inflammation-induced depressive-like behaviors via sigma-1 receptor delivery. *Brain Behav. Immun.* **94**, 225-234

80. Lu, X., Liu, H., Cai, Z., Hu, Z., Ye, M., Gu, Y., Wang, Y., Wang, D., Lu, Q., Shen, Z., Shen, X., and Huang, C. (2022) ERK1/2-dependent BDNF synthesis and signaling is required for the antidepressant effect of microglia stimulation. *Brain Behav. Immun.* **106**, 147-160

81. Sosicka, P., Ng, B. G., Pepi, L. E., Shajahan, A., Wong, M., Scott, D. A., Matsumoto, K., Xia, Z. J., Lebrilla, C. B., Haltiwanger, R. S., Azadi, P., and Freeze, H. H. (2022) Origin of cytoplasmic GDP-fucose determines its contribution to glycosylation reactions. *J. Cell Biol.* **221**

82. Lester, D. K., Burton, C., Gardner, A., Innamarato, P., Kodumudi, K., Liu, Q., Adhikari, E., Ming, Q., Williamson, D. B., Frederick, D. T., Sharova, T., White, M. G., Markowitz, J., Cao, B., Nguyen, J., Johnson, J., Beatty, M., Mockabee-Macias, A., Mercurio, M., Watson, G., Chen, P. L., McCarthy, S., MoranSegura, C., Messina, J., Thomas, K. L., Darville, L., Izumi, V., Koomen, J. M., Pilon-Thomas, S. A., Ruffell, B., Luca, V. C., Haltiwanger, R. S., Wang, X., Wargo, J. A., Boland, G. M., and Lau, E. K. (2023) Fucosylation of HLA-DRB1 regulates

CD4(+) T cell-mediated anti-melanoma immunity and enhances immunotherapy efficacy. *Nat. Cancer* **4**, 222-239

83. Etzioni, A., and Tonetti, M. (2000) Fucose supplementation in leukocyte adhesion deficiency type II. *Blood* **95**, 3641-3643

84. Marquardt, T., Lühn, K., Srikrishna, G., Freeze, H. H., Harms, E., and Vestweber, D. (1999) Correction of leukocyte adhesion deficiency type II with oral fucose. *Blood* **94**, 3976-3985

85. Hsu, H. Y., and Hwang, P. A. (2019) Clinical applications of fucoidan in translational medicine for adjuvant cancer therapy. *Clin. Transl. Med.* **8**, 15

86. Lin, Y., Qi, X., Liu, H., Xue, K., Xu, S., and Tian, Z. (2020) The anti-cancer effects of fucoidan: a review of both in vivo and in vitro investigations. *Cancer Cell Int.* **20**, 154

87. Wang, Y. Q., Wei, J. G., Tu, M. J., Gu, J. G., and Zhang, W. (2018) Fucoidan Alleviates Acetaminophen-Induced Hepatotoxicity via Oxidative Stress Inhibition and Nrf2 Translocation. *Int. J. Mol. Sci.* **19**

88. Saitoh, Y., Nagai, Y., and Miwa, N. (2009) Fucoidan-Vitamin C complex suppresses tumor invasion through the basement membrane, with scarce injuries to normal or tumor cells, via decreases in oxidative stress and matrix metalloproteinases. *Int. J. Oncol.* **35**, 1183-1189

89. Vishchuk, O. S., Ermakova, S. P., and Zvyagintseva, T. N. (2013) The effect of sulfated (1→3)-α-l-fucan from the brown alga Saccharina cichorioides Miyabe on resveratrol-induced apoptosis in colon carcinoma Cells. *Mar. Drugs* **11**, 194-212

90. Hsu, H. Y., Lin, T. Y., Hu, C. H., Shu, D. T. F., and Lu, M. K. (2018) Fucoidan upregulates TLR4/CHOP-mediated caspase-3 and PARP activation to enhance cisplatin-induced cytotoxicity in human lung cancer cells. *Cancer Lett.* **432**, 112-120

91. Shannon, E., Conlon, M., and Hayes, M. (2021) Seaweed Components as Potential Modulators of the Gut Microbiota. *Mar. Drugs* **19**

92. van Weelden, G., Bobiński, M., Okła, K., van Weelden, W. J., Romano, A., and Pijnenborg, J. M. A. (2019) Fucoidan Structure and Activity in Relation to Anti-Cancer Mechanisms. *Mar. Drugs* **17**

93. Guo, C., Yang, L., Wan, C. X., Xia, Y. Z., Zhang, C., Chen, M. H., Wang, Z. D., Li, Z. R., Li, X. M., Geng, Y. D., and Kong, L. Y. (2016) Anti-neuroinflammatory effect of Sophoraflavanone G from Sophora alopecuroides in LPS-activated BV2 microglia by MAPK, JAK/STAT and Nrf2/HO-1 signaling pathways. *Phytomedicine* **23**, 1629-1637

94. Zeng, K. W., Wang, S., Dong, X., Jiang, Y., and Tu, P. F. (2014) Sesquiterpene dimer (DSF-52) from Artemisia argyi inhibits microglia-mediated neuroinflammation via suppression of NF-κB, JNK/p38 MAPKs and Jak2/Stat3 signaling pathways. *Phytomedicine* **21**, 298-306

95. Zhang, M., Sui, W., Cheng, C., Xue, F., Tian, Z., Cheng, J., Zhang, J., Zhang, T., Zhang, J., Wang, W., Xiong, W., Hao, P., Ma, J., Xu, X., Wang, S., Sun, S., Zhang, M., Zhang, Y., and Zhang, C. (2021) Erythropoietin promotes abdominal aortic aneurysms in mice through angiogenesis and inflammatory infiltration. *Sci. Transl. Med.* **13**

96. Ben-Ali, M., Ben-Khemis, L., Mekki, N., Yaakoubi, R., Ouni, R., Benabdessalem, C., Ben-Mustapha, I., and Barbouche, M. R. (2019) Defective glycosylation leads to defective gp130-dependent STAT3 signaling in PGM3-deficient patients. *J. Allergy Clin. Immunol.* **143**, 1638-1640.e1632

97. Waetzig, G. H., Chalaris, A., Rosenstiel, P., Suthaus, J., Holland, C., Karl, N., Vallés Uriarte, L., Till, A., Scheller, J., Grötzinger, J., Schreiber, S., Rose-John, S., and Seegert, D. (2010) N-

linked glycosylation is essential for the stability but not the signaling function of the interleukin-6 signal transducer glycoprotein 130. *J. Biol. Chem.* **285**, 1781-1789

98. Banerjee, S., Biehl, A., Gadina, M., Hasni, S., and Schwartz, D. M. (2017) JAK-STAT Signaling as a Target for Inflammatory and Autoimmune Diseases: Current and Future Prospects. *Drugs* **77**, 521-546

99. Hong, S., Feng, L., Yang, Y., Jiang, H., Hou, X., Guo, P., Marlow, F. L., Stanley, P., and Wu, P. (2020) In Situ Fucosylation of the Wnt Co-receptor LRP6 Increases Its Endocytosis and Reduces Wnt/β-Catenin Signaling. *Cell Chem. Biol.* **27**, 1140-1150.e1144

100. Shami Shah, A., Sun, H., and Baskin, J. M. (2020) For Wnt Signaling, Fucosylation of LRP6 Is a Bitter Pill. *Cell Chem. Biol.* **27**, 1114-1116

101. Freimoser-Grundschober, A., Rueger, P., Fingas, F., Sondermann, P., Herter, S., Schlothauer, T., Umana, P., and Neumann, C. (2020) FcγRIIIa chromatography to enrich a-fucosylated glycoforms and assess the potency of glycoengineered therapeutic antibodies. *J. Chromatogr. A* **1610**, 460554

102. Sakae, Y., Satoh, T., Yagi, H., Yanaka, S., Yamaguchi, T., Isoda, Y., Iida, S., Okamoto, Y., and Kato, K. (2017) Conformational effects of N-glycan core fucosylation of immunoglobulin G Fc region on its interaction with Fcγ receptor IIIa. *Sci. Rep.* **7**, 13780

6. Abbreviations

Akt: protein kinase B

CNS: central nervous system

CRISPR/Cas-9: clustered regularly interspaced short palindromic repeats/caspase-9

DG: dentate gyrus

Fut8: α1,6-fucosyltransferase

gp130: glycoprotein 130

Iba-1: ionized calcium-binding adaptor molecule-1

iNOS: inducible nitric oxide synthase

IL-1β: interleukin-1β

IL-6: interleukin-6

IVIS: *in vivo* imaging system

JAK2: Janus kinase 2

LCA: *Lens Culinaris Agglutinin*

LPS: lipopolysaccharide

Luc: luciferase

MS: mass spectrometry

PI3K: phosphoinositide 3-kinase

sIL-6R: soluble IL-6 receptor

STAT3: signal transducer and activator of transcription 3

TNF-α, tumor necrosis factor-alpha

7. Acknowledgments

The three years and three months at the Tohoku Medical and Pharmaceutical University is a pivotal and memorable experience in my life. I want to extend my sincere thanks to all those who have supported, encouraged, and assisted me.

Firstly, I want to express my deepest appreciation to President Motoaki Takayanagi for granting me the opportunity to pursue my studies at Tohoku Medical and Pharmaceutical University and for providing financial support.

Secondly, I consider myself incredibly fortunate to have had the honor of being guided by Professor Jianguo Gu. His profound insights and enlightened guidance have played an indispensable role in my journey of acquiring new knowledge and ultimately completing my studies.

I also would like to express my deep appreciation to Dr. Tomohiko Fukuda for his invaluable guidance and technical assistance. Many thanks for Dr. Tomoya Isaji providing experimental helps. Additionally, I wish to present my appreciation to Ms. Yan Hao and Ms. Yuhan Sun for their assistance and encouragement.

Thirdly, I would like to extend my heartfelt gratitude to my beloved family for their thoughtful concern and continual encouragement, which has been a pillar of strength and motivation throughout my endeavors. Their unwavering support has been a constant source of inspiration, and I am truly thankful for the invaluable role they have played in my PhD journey.

Finally, I extend my appreciation to myself for the perseverance and hard work that have been instrumental in reaching this significant academic milestone. I am genuinely proud of the strides I have made in the pursuit of knowledge and achievement.